Article:
Scarfone, R., Wheeler, S.J. and Smith, C.C. (2023) Numerical modelling of the application of capillary barrier systems for prevention of rainfall-induced slope instability. Acta Geotechnica, 18 (1). pp. 355-378. ISSN: 1861-1125

https://doi.org/10.1007/s11440-022-01582-w

Numerical modelling of the application of Capillary Barrier Systems for prevention of rainfall-induced slope instability

Author 1*

- Riccardo Scarfone, PhD, Geotechnical Engineer
- Geotechnical Consulting Group, London, United Kingdom. Formerly: James Watt School of Engineering, University of Glasgow, Glasgow, United Kingdom
- https://orcid.org/0000-0003-0268-9537
- r.scarfone@gcg.co.uk

***Corresponding author.**

Author 2

- Simon J. Wheeler, Cormack Professor of Civil Engineering
- James Watt School of Engineering, University of Glasgow, Glasgow, United Kingdom
- https://orcid.org/0000-0003-1493-2434
- Simon.Wheeler@glasgow.ac.uk

Author 3

- Colin C. Smith, PhD, Senior Lecturer
- Department of Civil and Structural Engineering, University of Sheffield, Sheffield, United Kingdom
- https://orcid.org/0000-0002-0611-9227
- c.c.smith@sheffield.ac.uk

Article type: Original Research Paper
Number of words in the main text: 9766
Number of figures: 17
Number of tables: 3

Abstract

The most common cause of slope instability is intense or sustained rainfall, which may induce reduction in soil suction, and thus shear strength. Capillary Barrier Systems (CBSs) can be used to prevent rainwater infiltration into the underlying soil and thus prevent slope instability. The application of CBSs for prevention of slope instability was studied by means of advanced 2D thermo-hydraulic finite element simulations and limit analyses. The roles of materials and thickness of the CBS, slope height and weather conditions were investigated. Climatic conditions of dry and warm (Cagliari, Italy) and wet and cool (London, UK) European areas were simulated. Sloping CBSs having the finer layer made of finer-grained materials, such as silty sand, were proven to be more effective in regions with warm

and dry climates (with occasional intense rainfall events), because their key working mechanism is water storage, whereas sloping CBSs having the finer layer made of slightly coarser-grained materials, such as fine sand, are effective under a wider range of climatic conditions, because their key working mechanism is lateral water diversion. The effectiveness of CBSs was found to decrease with increasing slope height. However, two solutions were proven to be effective at widening the range of applicability of CBSs to higher slopes: multi-layered CBSs and multiple drains. All the CBSs analyzed were proven to be effective at preventing rainfall-induced slope instability.

Keywords

Capillary barriers; Slope stability; Suction; Numerical modelling; Rainfall; Soil-atmosphere interaction.

Declarations

Funding. This work was supported by the European Commission via the Marie Skłodowska-Curie Innovative Training Networks (ITN-ETN) project TERRE 'Training Engineers and Researchers to Rethink geotechnical Engineering for a low carbon future' (H2020-MSCA-ITN-2015-675762).

Conflicts of interest/Competing interests. The authors have no conflicts of interest to declare that are relevant to the content of this article.

Availability of data and material. All data presented in this article will be made available upon acceptance of the paper in a repository online in accordance with funder data retention policies. The online repository will be the institutional repository ‘‘Enlighten’’ of the University of Glasgow.

Code availability. The codes used for the analyses, Code_Bright and LimitState:GEO, are publicly available for download.

Authors' contributions. Riccardo Scarfone: Conceptualization, Methodology, Formal analysis and investigation, Writing - original draft preparation. Simon J. Wheeler: Conceptualization, Methodology, Writing - review and editing, Resources, Supervision. Colin C. Smith: Methodology, Writing - review and editing, Supervision.

Acknowledgements

The authors wish to acknowledge the support of the European Commission via the Marie Skłodowska-Curie Innovative Training Networks (ITN-ETN) project TERRE 'Training Engineers and Researchers to Rethink geotechnical Engineering for a low carbon future' (H2020-MSCA-ITN-2015-675762).

1. Introduction

Under unsaturated conditions, the presence of soil suction s, defined as the difference between the pore-gas pressure p_g and the pore liquid pressure p_l, i.e. $s = p_g - p_l$, may impart significant gains in the shear strength of soils. According to the water retention behaviour of unsaturated soils, suction s always decreases with increasing degree of liquid saturation S_l. This means that the beneficial effect of suction may be lost or reduced during wetting events, such as intense or sustained rainfall, inducing an increase of S_l.

The stability of slopes, in particular those made of fine-grained materials with low values of friction angle, is often guaranteed by the presence of suction (Ng and Shi, 1998). Suction typically increases during dry and warm periods, thanks to the effect of evapotranspiration from the soil into the atmosphere, and decreases during rainfall events. After an intense and/or sustained rainfall event, the reduction in suction, and thus in shear strength, may be sufficient to cause slope instability (Ng and Shi, 1998). Intense or sustained rainfall is, in fact, the most common cause of landslides (Iverson, 2000; Polemio and Petrucci, 2000). The risk of rainfall-induced slope instability can be mitigated by preventing or limiting rainwater infiltration into the soil.

Capillary Barrier Systems (CBSs) are geotechnical structures made of an upper finer-grained layer (F.L.), typically ranging from fine sand to low plasticity silt, overlying a coarser-grained layer (C.L.), typically ranging from gravel to medium sand, placed above the natural soil to prevent or reduce the infiltration of rainwater into the underlying soil (U.S.) (Stormont and Anderson, 1999). The coarser layer is typically at very low degree of saturation and hence the corresponding unsaturated hydraulic conductivity, which decreases by many orders of magnitude with decreasing degree of saturation, is also very low. Thus, the coarser layer acts as an almost impermeable barrier and the rainwater is stored in the upper finer layer. The rainwater stored in the finer layer is then removed by evapotranspiration and/or lateral drainage down the slope. The coarser layer will continue to behave as an impermeable layer unless it reaches a critical condition (breakthrough), which typically corresponds to high degree of saturation of the finer layer (Stormont and Anderson, 1999). CBSs are often preferred to other soil covers for their low-cost (Dwyer, 1998), possibility to use recycled low-cost materials (Harnas et al., 2014) and high durability (Suter et al., 1993; Henken-Mellies and Schweizer, 2011; Morris and Stormont, 1998; Zhang, 2016).

The working principle of horizontal CBSs and the phenomenon of water breakthrough have been studied by several authors, both experimentally (Baker and Hillel, 1990; Stormont and Anderson, 1999; Yang et al., 2004a; Yang et al., 2004b; Yang et al., 2006) and numerically (Stormont and Morris, 1998; Khire et al., 2000; Scarfone et al. 2020a; Scarfone et al. 2020b). Similarly, many authors analysed the behaviour of sloping CBSs and their ability to divert rainwater laterally, theoretically (Ross, 1990; Steenhuis et al., 1991; Stormont, 1995), experimentally (Stormont, 1996; Pease and Stormont, 1996; Kämpf and Montenegro, 1997; Abdolahzadeh et al., 2011; Zhan et al., 2014) or numerically (Oldenburg and Pruess, 1993; Webb, 1997; Parent and Cabral, 2006; Lacroix Vachon et al., 2015).

CBSs have been traditionally used as landfill covers (Morris and Stormont, 1998). Their effectiveness for this purpose has been proved in arid and semi-arid climates, but they have been found to be less effective in preventing water percolation in humid climates (Morris and Stormont, 1999). In order to improve their effectiveness, different non-conventional CBSs have been proposed, such as CBSs with a drainage layer (Stormont and Morris, 1997), three-layer CBS with a compacted clay layer under a conventional CBS (Ng et al., 2016) and a dual CBS (Harnas et al., 2014).

Only relatively recently, have CBSs started to be seen as a means to control suction in the ground, with particular application to slope stability (Rahardjo et al., 2011). CBSs were proven to be effective for prevention of rainfall-induced slope instability by Rahardjo et al. (2007, 2011, 2013) by means of three field tests in three different areas of Singapore at risk of rainfall-induced slope instability. They showed that higher suction values were maintained during rainfall in slopes covered by CBSs compared to bare slopes, resulting in a higher factor of safety. Harnas et al. (2016) analysed numerically a particular case study comparing the performance of a bare slope, a slope covered by a standard CBS and a slope covered by a dual CBS. They showed that the use of either type of barrier reduced the risk of slope instability and that the dual capillary barrier was the most effective at maintaining suction in the original soil.

Although recent studies showed the potential of CBSs for slope stability purposes, further research on this topic is still required. When the behaviour of CBSs has been analysed numerically, this has typically involved very simplified analyses, e.g. poor description of the hydraulic behaviour at low degree of

saturation, no consideration of water retention hysteresis and poor modelling of soil atmosphere-interaction, and the role of the different problem parameters, such as geometry, materials and weather conditions, has not been clearly analysed. Different researchers have tried to extend the applicability of CBSs from arid or semi-arid to wetter climatic areas, such as Hong Kong (Ng et al., 2015), Singapore (Rahardjo et al., 2016) and some regions of China (Zhang et al., 2016). Although these areas are characterised by high amounts of yearly rainfall, they are however also characterised by high evaporation rates due to high temperatures.

In the current work, these gaps in existing knowledge were addressed by performing advanced numerical analyses (finite element and limit analysis) investigating the long-term performance of CBSs when used for prevention of rainfall induced slope instability and the role of the various key parameters. These analyses included a comparison between the modelling results for two contrasting European climatic conditions, a dry and warm climate, with occasional intense rainfall events, represented by Cagliari (Italy), and wet and cool climatic conditions, represented by London (UK), characterised by high amount of rainfall and low evaporation. Solutions aimed to improve the effectiveness of the application of CBSs to prevent slope instability were also analysed, such as the use of multiple drains and multi-layered CBSs.

2. Working mechanisms of Capillary Barrier Systems: water storage and lateral diversion

The hydraulic behaviour of CBSs and their ability to prevent rainwater percolation are governed by the water balance in the finer layer. The rainwater entering the top of the CBS is stored in the finer layer thanks to the capillary barrier effect created at the interface with the C.L.. This water can be removed by evapotranspiration and/or lateral drainage if the CBS is sloped. Therefore, two main working mechanisms can be identified for horizontal and sloping CBSs, as shown in Fig. 1.

Fig. 1a shows the typical working mechanism of a horizontal CBS. When it rains, the rainwater is stored in the F.L., while the C.L., typically at low degree of saturation and thus at very low unsaturated hydraulic conductivity, acts as an almost impermeable layer, preventing the water stored in the F.L. from percolating downwards. During periods when it is not raining, water is extracted from the F.L. by means of evapotranspiration, which hence causes a decrease of the degree of saturation and an increase of suction within the F.L. However, if an excessive amount of water enters the finer layer during a rainfall

event, exceeding the water storage capacity of the CBS (Stormont and Morris, 1998), water breakthrough from the F.L. into the C.L. will occur, causing percolation eventually into the underlying soil. Water breakthrough across the interface between F.L. and C.L. occurs when the suction at the interface decreases down to the "bulk water continuity" (BWC) value of the coarser layer, which is the suction value at which the hydraulic conductivity of the coarser layer starts increasing dramatically (Scarfone et al., 2020a).

In addition to evapotranspiration, rainwater can be extracted from the finer layer of sloping CBSs by lateral diversion down the slope, driven by gravity, as shown in Fig. 1b. At the top of the slope, infiltrating water starts entering the finer layer, suction at the interface between finer and coarser layers is relatively high since the water content is low, the coarser layer behaves as an impermeable layer and water is diverted laterally down the slope within the finer layer due to the effect of gravity. Moving down the slope, the amount of water flowing laterally within the finer layer increases. To achieve this, the degree of saturation at the base of the finer layer is greater than that further up the slope, and the suction at the interface is correspondingly lower. If the suction at the interface decreases down to a point where suction equals the BWC value of the coarser layer, the coarser layer becomes highly hydraulically conductive (breakthrough occurs). Beyond that point, no more water, in addition to that already diverted from further up the slope, can be diverted laterally, because the lateral diversion capacity is already fully attained. Infiltrating water therefore becomes percolation into the coarser layer, i.e. in the lower part of the slope the percolation into the coarser layer is equal to the rainfall infiltration rate (Ross, 1990). The "diversion length" L_D of the barrier is the horizontal distance from the top of the slope to the point down the slope where breakthrough commences and the "diversion capacity" $Q_{D,max}$ is the flow rate across vertical cross-sections of the finer layer from this point onwards (see Fig.1b).

3. Numerical methodology and models

3.1 Numerical methodology

Various numerical analyses were performed in this work in order to analyse the long-term performance of CBSs applied to slopes subject to realistic weather conditions, with particular focus on the hydraulic response of the CBSs and the underlying soil and the effect on slope stability. The modelling procedure adopted in this work can be divided into the following three steps:

1) Advanced two-dimensional finite element (FE) coupled thermo-hydraulic analyses were performed by means of the software Code_Bright (Olivella et al., 1996) modelling multi-phase and multi-physics processes. Thermal modelling was required, in addition to hydraulic modelling, because of the inclusion of evaporation from the slope surface to the atmosphere and vapour transfer within the soil. Concerning the mass balance, advective liquid flow and diffusion of water vapour within the gas phase were modelled by means of Darcy's law and Fick's law respectively. Advective gas flow was neglected and gas pressure was considered uniform and constant in the model, equal to the atmospheric pressure, p_g =100 kPa. Concerning the energy balance, conductive heat flow was modelled by means of Fourier's law. Convective heat flow (i.e. heat flux associated to mass fluxes of liquid and vapour) was also included. The mechanical behaviour of the materials was assumed to be rigid in the FE analyses. Realistic weather conditions were considered through the advanced modelling of soil-atmosphere interaction. The results of these analyses in terms of temporal and spatial variations of suction s and degree of saturation S_l at the nodes of the FE mesh were exported to a link code.
2) A link code was developed *ad hoc* with the aim of importing the nodal values of s and S_l from the FE model at different times and interpolating the values of the product $s \cdot S_l$ to a new grid. Further details about the link code are provided by Scarfone (2020).
3) The new grid values of the product $s \cdot S_l$, which had a key role in modelling the shear strength of the unsaturated soils, as described later, were subsequently exported into computational limit analysis (LA) software LimitState:GEO (LimitState, 2019) to perform stability analysis at different critical times considering the effect of unsaturated conditions on shear strength. A discontinuity layout optimization method (Smith and Gilbert, 2007) is used in the software to identify potential failure mechanisms and the corresponding factors of safety.

3.2 Geometry

Various two-dimensional geometries were considered in the numerical analyses, as shown in Fig. 2 in which the numerical FE meshes are presented.

In two models (Figs. 2a and 2b), only the underlying soil was considered. In both cases, the angle of the slope was 35°. As an indicative rule, CBSs are potentially useful for slope stability purposes if the slope angle lies between the friction angle of the underlying soil (i.e. 20° in these analyses) and the

friction angle of the materials of the CBS (35° to 40° in these analyses). For slope angles lower than the friction angle of the underlying soil, the slope is likely to be stable without a CBS, even after intense rainfall, whereas for slope angles greater than the friction angle of the CBS materials, even a slope covered by a CBS is likely to be unstable. Two slope heights were considered: H_s = 6m (Fig. 2a) and H_s = 10m (Fig. 2b). Lateral and bottom boundaries were located at sufficient distance that the behaviour of the slope was not affected by the position of the boundaries.

Different models in which a CBS covers the slope surface were analysed, shown in Figs. 2c-g. In all these models, the underlying slope was identical either to the model shown in Fig. 2a or to that shown in Fig. 2b. Figs. 2c-g only show a zoomed view of the central part of the model, where the slope is covered by a CBS. In the model shown in Fig. 2c, the 6m-high slope presented in Fig. 2a was covered by a sloping CBS of a total thickness of t_{CBS} = 60cm, measured perpendicular to the slope. In the models shown in Figs. 2d and 2e, the 10m-high slope presented in Fig. 2b was covered by sloping CBSs of a total thickness of t_{CBS} = 60cm and t_{CBS} = 100cm, respectively. The coarser layer of the CBSs was 20cm thick in all models whereas the finer layer was either 40cm thick (for t_{CBS} = 60cm) or 80cm thick (for t_{CBS} = 100cm). The thickness of the C.L. does not affect the response of the CBS, provided it is higher than the minimum value suggested by Yang et al (2004b) (approximately 2cm in this case) and its value (20cm) was chosen as the minimum that might be realistically adopted on site without leading to significant tolerance defects. The values of the thickness of the F.L. were chosen as the lower bound (40cm) and the upper bound (80cm) that are typically adopted on site for construction of a CBS. The slopes were totally covered by the CBSs and at the top and at the toe the CBSs also covered the horizontal soil surface for a short length, of approximately 1.3m.

The application of a non-conventional CBS, such as a multi-layered Capillary Barrier (MCB), was also analysed when applied to the 10m-high slope (see Fig. 2f). The MCB was made of two coarser layers and two finer layers. The finer layers were 27.5cm thick, the intermediate coarser layer was 5cm thick and the bottom coarser layer was 20cm thick, for a total thickness of t_{CBS} = 60cm. The various FE meshes used for all the different models employed 8 to 26 elements through the thickness of each layer of a CBS or MCB, with element thicknesses perpendicular to the slope reduced in proximity to any interface (with another material or the ground surface).

The presence of a drain was modelled at the toe of all the slopes covered by a CBS (Figs. 2c-g) in order to collect the water potentially diverted laterally down the slope by the CBSs. In the model shown in Fig. 2g, in addition to the bottom drain, the presence of an intermediate drain located at the mid-height of the slope was modelled to assess the effect of the presence of multiple drains on the hydraulic response of the slope and its stability. A conventional CBS with a thickness of t_{CBS} = 60cm applied to a 10m-high slope was considered for this model. In reality, these drains are perforated tubes running sub-horizontally in the longitudinal direction of the slope (i.e. in the out-of-plane direction of the 2-D model), collecting water diverted from the F.L. and taking it to a collection point further along the slope. In the numerical FE models, the drains were modelled by applying appropriate surface conditions to some specific mesh elements in the coarser layer, whose location is highlighted by the dashed line in Fig. 2g. These drainage surface boundary conditions can be seen as a surface liquid water outflow occurring orthogonal to the 2D plane. No drainage occurs if the suction is higher than s^c_{BWC} whereas the suction value s^c_{BWC} is imposed at the nodes of these elements if suction attains this value, where s^c_{BWC} is the bulk water-continuity value of suction of the coarser layer (in this case $s^c_{BWC} \approx$ 0.2kPa). In this way, water is drained away from the model once it flows from the F.L. into the C.L. in the areas where drains are modelled.

The geometries of the LA models analysed with LimitState:GEO coincided with those of the FE models analysed with Code_Bright.

3.3 Materials

Four materials were considered in this study. The material properties adopted for the underlying soil (U.S.) and for the coarser layer (C.L.) of the CBS were respectively representative of a silt and a gravelly sand. Two types of material were considered for the finer layer (F.L.), with properties representative of a fine sand or a silty sand. From the comparison of the results obtained considering these two materials, it was possible to assess the role of the material properties of the F.L. on the response of the system. The soil water retention curve (SWRC), relating degree of saturation S_l and suction s, and the soil hydraulic conductivity curve (SHCC), relating the unsaturated hydraulic conductivity k_l and suction s, of the materials modelled in the analyses are shown in Fig. 3. Table 1 and Table 2 respectively show the material properties adopted in the FE analyses and in the limit analyses. Material properties of the fine sand (one of the two F.L materials) and the gravelly sand (the C.L

material) were referenced to experimental data by Yang et al (2004a, 2004b), whereas those of the silty sand (the other F.L. material) and the silt were hypothetical but typical of relevant materials from the literature.

The hydraulic behaviour of the materials (SWRC and SHCC) was modelled using an advanced constitutive model developed by Scarfone et al (2020a), who improved the van Genuchten (1980) and Mualem (1976) models at very low degree of saturation, including consideration of the contribution of adsorbed liquid films to hydraulic conductivity. Scarfone et al (2020a) showed that modelling the effect of adsorbed liquid film flow in the hydraulic conductivity is very important for accurate modelling of the phenomenon water breakthrough from the F.L. into the C.L. Hydraulic hysteresis was also included using the bounding surface based model developed by Scarfone et al (2020b). The vapour diffusivity and the thermal conductivity were respectively modelled by Fick's law and Fourier's law. The material constitutive equations adopted in the FE analyses are shown in Table 1. Default laws and parameters implemented in Code_Bright were used for the modelling of physical properties (e.g. liquid viscosity, liquid density, gas density and vapour mass fraction in the gas phase).

Rigid-perfectly plastic behaviour was assumed for all materials in the limit analyses, with Mohr-Coulomb yield criterion and associative plastic flow. The material parameters for these analyses were the unit weight γ, the friction angle ϕ' and the effective cohesion c', with the parameter values adopted shown in Table 2. The values adopted for the unit weight reflect the porosity, the specific gravity of the soil particles and the range of degree of saturation expected during intense rainfall events. The friction angle values used for the materials of the CBSs, i.e. fine sand, silty sand and gravelly sand, are close to the upper bounds of the range of possible values for these materials (Swiss Standard SN 670 010b, 1999), corresponding to a high relative density state, as a result of the expected compaction on site. A relatively low value of friction angle was used to represent the silt (Swiss Standard SN 670 010b, 1999), which represents a natural material already present on site. A small value of effective cohesion (i.e. c' = 0.1kPa) was assigned to all materials in order to avoid numerical instabilities. No specific shear strength properties were imposed at the interfaces between different layers and, consequently, the shear strength at each interface was the lower of those exhibited by the two layers.

Within the limit analyses, unsaturated conditions were considered in the yield criterion using the Bishop (1959) stress with $\chi = S_l$ which, although it is not capable of representing all aspects of the mechanical behaviour of unsaturated soils, is adequate to model the shear strength (Gallipoli et al, 2008). The yield criterion can be thus expressed as:

$$\tau = c' + \left(\sigma - p_g + s \cdot S_l\right) \cdot \tan \phi' \quad (1)$$

where τ is the shear strength exhibited along a specific failure surface and σ is the normal total stress acting perpendicular to the same failure surface. Equation 1 correctly converts to the standard saturated expression (Mohr-Coulomb, with $\sigma - p_l$ as the effective stress) when $S_l = 1$, irrespective of the value of s at which this occurs.

3.4 Initial and boundary conditions

The response of the models in the long-term was analysed when subjected to the application of realistic atmospheric conditions. Soil-atmosphere interaction was modelled by means of the application of an "atmospheric" boundary condition at the top of the FE models. For the mass transfer, this boundary condition included: rain P, runoff R (occurring when p_l at the boundary is equal to the atmospheric gas pressure) and evaporation E. The role of transpiration related to the presence of vegetation was not considered in this study. For the energy transfer, it included: radiation R_n, sensible heat flux (advection) H_s and latent heat flux H_c (convection).

The evaporation E was modelled as (Brutsaert, 1982):

$$E = \frac{k^2 v_a \psi}{\ln\left(\frac{z_a}{z_0}\right)^2} (\rho_v - \rho_{va}) \quad (2)$$

where k is the Von Karman's constant ($k = 0.4$), z_a is the screen height (in this work $z_a = 1.5$m), z_0 is the roughness length ($z_0 = 0.001$m in this work, valid for a surface covered by short grass), ψ is the stability factor ($\psi = 1$), v_a is the wind speed at the screen height, ρ_{va} is the absolute humidity of the atmosphere at the screen height and ρ_v is the absolute humidity at the boundary (soil surface). ρ_{va} is a function of the atmospheric temperature T_a, the relative humidity RH_a and the atmospheric gas pressure p_{ga}, whereas ρ_v is a function of temperature T, pore-liquid pressure p_l and pore-gas pressure p_g at the boundary (soil surface). These relationships are governed by the psychrometric law.

The sensible heat flux H_s was modelled as (Brutsaert, 1982):

$$H_s = \frac{k^2 v_a \psi}{\ln\left(\frac{z_a}{z_0}\right)^2} \rho_{ga} C_a (T_a - T) \quad (3)$$

where ρ_{ga} is the atmospheric gas density (ρ_{ga} = 1.2kg/m^3), C_a is the specific heat of the gas, T_a is the atmospheric temperature at the screen height and T is the temperature at the boundary (soil surface).

Two different climatic conditions were considered for this study: Cagliari (Italy), representative of a dry and warm European climatic area but subjected to sporadic intense rainfall events, and London (UK), representative of a wet and cool European climatic area. Historical data for the weather in Cagliari were obtained from the meteorological office of the Italian air force (Servizio metereologico Aeronautica Militare) whereas data for the weather in London were obtained from the meteorological office of the UK Government (Met Office). The atmospheric data processed for the modelling of the atmospheric boundary conditions were air temperature T_a, wind speed v_a, atmospheric relative humidity RH_a, cloud index I_n, radiation R_n and precipitation P. Cloud index I_n and radiation R_n are parameters important for the energy balance at the top atmospheric boundary (Olivella et al, 2021) and they affect the surface temperature and hence the evaporation. The average monthly values of the atmospheric parameters were calculated for years 1981-2010 and they are represented by the histograms in Figs. 4a-l. These data were then fitted by sinusoidal distributions adopted for the modelling of atmospheric conditions in Code_Bright, as shown by the solid lines in Figs. 4a-l. Figs. 4m and 4n show the daily amount of rainfall recorded respectively in Cagliari and London for particularly wet 10-year periods, i.e. 1984-1993 for Cagliari and 1993-2002 for London. The most critical rainfall event in Cagliari consisted of a daily rainfall of 73.8mm on 7th of March 1985, (t = 1.18274years in the analyses), whereas the most critical rainfall event in London consisted of a daily rainfall of 63.4mm on 1st of January 1998 (t = 5.00214years in the analyses), after a particularly wet period. Results will be shown at the end of these particular critical rainfall events.

The atmospheric parameters related to the energy transfer and evaporation (i.e. T_a, v_a, RH_a, I_n and R_n) varied according to the yearly sinusoidal distributions shown in Figs. 4a-j throughout the analyses. By contrast, the application of rainfall varied in three different analysis stages:

1) In stage 1, lasting 20 years, the CBS was not built yet and the yearly sinusoidal distributions of rainfall shown in Figs. 4k and 4l were applied to the underlying soil surface.

2) In stage 2, lasting 10 years, the CBS was constructed (in the models including a CBS) and the yearly sinusoidal distributions of rainfall shown in Figs. 4k and 4l were applied to the surface of the CBS. In the models with the bare slope (see Figs. 2a and 2b), this stage consisted of a repetition of the first stage for a further 10 years.
3) In the third stage, lasting 10 years, rain was applied to the soil surface (either underlying soil or CBS) using the daily rainfall data shown in Figs. 4m and 4n.

Stages 1 and 2 were preliminary stages needed to set up realistic initial distributions of s, S_l and T respectively in the underlying soils and in the CBS after construction (in the models in which a CBS was present). Stage 3 was used to analyse the response of the models to more accurate time histories of rainfall, characterised by a particularly wet 10-year sequence of recorded daily data. The results of interest for this work, shown in the subsequent sections, are those obtained during stage 3.

The lateral boundaries were modelled as impermeable to liquid and heat flows in all FE models. For the weather of Cagliari, the bottom boundary was modelled as impermeable to liquid and heat flows. For the weather of London, the bottom boundary was modelled as impermeable to heat flow but a constant pore-liquid pressure of p_l = 0.247MPa (i.e. a positive pore liquid pressure of 0.147MPa above atmospheric pressure) was applied, corresponding to a position of the water table 5m below the base of the slope in hydrostatic conditions.

The lateral and bottom boundaries of the limit analysis models were fixed, that is only displacements parallel to the boundary were permitted. The top boundaries were modelled as free, meaning that movements both parallel and perpendicular to the boundaries were permitted.

Further details of the numerical models are described by Scarfone (2020). Preliminary numerical tests were performed to ensure the accuracy of all aspects of the various numerical models (e.g. mesh, modelling of drains, boundary conditions, etc.).

4. Results of the analyses

This section presents the results of the two-dimensional FE thermo-hydraulic analyses of slopes and limit analyses for slope stability. Fourteen different simulations were performed combining different weather conditions, materials and thicknesses of the finer layer and slope heights. In addition, the

effects of the use of multiple drains across the slope and the use of multi-layered CBSs were investigated. The list of these fourteen two-dimensional analyses is shown in Table 3. The comparisons of the results obtained from different simulations highlight the general role of a CBS applied for slope protection and the roles of the different key parameters and conditions.

4.1 Effect of slope height

The effect of slope height is illustrated by comparing the results obtained for slope heights of H_s = 6m and H_s = 10m for the weather conditions of Cagliari. For each case, the bare slope and the slope covered by a CBS were analysed. The form of the CBS selected for this illustration is a single CBS with the F.L. made of fine sand and with t_{CBS} = 60cm. The results of the following models are shown: Cag_6_NOCBS, Cag_6_SCB_FS_60_SD, Cag_10_NOCBS and Cag_10_SCB_FS_60_SD.

Fig. 5 shows, for the different models, contours of degree of saturation and suction from the upper part of the FE mesh at the end of the most critical rainfall event. In both models with no CBS (Figs. 5a and 5c), a wetting front propagated downwards into the underlying soil from the surface. Above this wetting front, which was approximately 80cm deep at the end of the most critical rainfall event, the soil was fully saturated and the suction attained very low values, approaching 0 at the surface. Below the wetting front, the soil was at low degree of saturation ($S_l \approx 0.27$) and high values of suction. In the presence of the CBS on the slope with H_s = 6m (Fig. 5b), the soil under the footprint of the CBS was maintained at lower degree of saturation and higher suction even during the most critical rainfall event, unlike the lateral areas at the top and bottom of the slope not covered by the CBS. The CBS efficiently diverted the rainwater down the slope to the bottom drain. A similar pattern can be observed for the slope with H_s = 10m (Fig. 5d). However, in this case, breakthrough occurred into the C.L. and into the underlying soil close to the toe of the slope, causing an increase of the degree of saturation and decrease of suction in a small area of the underlying soil under the footprint of the CBS.

A similar conclusion can be drawn by observing Fig. 6 showing the time histories of suction s and degree of saturation S_l in the underlying soil at the toe of the slopes (see the location of points A in Fig. 5) for the four models. In the absence of a CBS, s and S_l fluctuated depending on the weather conditions, attaining full saturation and very low values of suction during extreme rainfall events. In the presence of a CBS on the 6m-high slope (Figs. 6a and 6c), the magnitude of these fluctuations was controlled

and relatively high values of suction and low values of degree of saturation were always maintained, even during rainfall. The CBS applied to the 10m-high slope was able to prevent rainwater infiltration into the underlying soil for most of the time. However, water breakthrough occurred at the toe of the slope on two occasions, as shown by the peaks in degree of saturation and low values of suction attained by the dashed curves in Figs. 6b and 6d.

The same CBS under the same weather conditions led to water breakthrough into the underlying soil at the toe when applied to a slope with a height of H_s = 10m whereas it did not cause any water breakthrough when applied to a slope with a height of H_s = 6m. In the two cases the diversion length was the same. However, unlike the 6m-high slope, in the 10m-high slope the horizontal distance between the top of the slope and the bottom drain is greater than the diversion length of the CBS. This demonstrates that, if the main working mechanism of a conventional CBS is lateral water diversion down the slope, the CBS will be effective for relatively small slopes but may not be fully effective in protecting tall slopes. Nevertheless, alternative ways to extend the application of CBSs to tall slopes, such as multi-layered CBSs and the use of multiple drains, are discussed in subsequent sections.

4.2 Effect of thickness and materials of the CBS and weather conditions

Different models were analysed considering different thicknesses of the CBS (t_{CBS} = 60cm and t_{CBS} = 100cm), different materials of the finer layer of the CBS (fine sand and silty sand) and different weather conditions (Cagliari and London). The corresponding bare slopes were also analysed. For all these models, the slope height was H_s = 10m and only a single drain at the toe was modelled. The results of the following models are presented in this section: Cag_10_NOCBS, Cag_10_SCB_FS_60_SD, Cag_10_SCB_FS_100_SD, Cag_10_SCB_SS_60_SD, Cag_10_SCB_SS_100_SD, Lon_10_NOCBS, Lon_10_SCB_FS_60_SD, Lon_10_SCB_FS_100_SD, Lon_10_SCB_SS_60_SD, Lon_10_SCB_SS_100_SD.

Fig. 7 shows the suction contours for the various models at the end of the most critical rainfall events. In the absence of a CBS (Figs. 7a and 7f), the soil near the surface, down to a depth of approximately 0.8m for Cagliari and between 1.7m and 3m for London, was fully saturated and the suction attained very low values approaching zero for the most critical rainfall events of both Cagliari and London. In the presence of the different CBSs (Figs. 7b-e and 7g-j), higher values of suction were maintained in the

soil underlying the CBSs even at the end of the most critical rainfall event, unlike the lateral zones at the top and bottom of the slope not covered by the CBS. However, in the part of the slope close to the toe, breakthrough occurred into the C.L. and into the underlying soil in some models (see Figs. 7b, 7c, 7d, 7g and 7i), causing a decrease of suction in very small areas of the underlying soil under the footprint of the CBSs. Exceptions were the models with the CBS having the F.L. made of silty sand and a thickness of t_{CBS} = 100cm for both Cagliari and London (Figs. 7e and 7j) and the CBS having the F.L. made of fine sand and a thickness of t_{CBS} = 100cm for London (Fig. 7h), in which no water breakthrough occurred throughout the simulation, even at the toe of the slope.

The impact of the CBSs on the hydraulic response of the underlying soil over time can be better understood by observing Fig. 8, which shows the time histories of suction obtained in the underlying soil at points A (toe), B (middle) and C (top) (see Fig. 7 for the locations of these points). Note that for the London weather (Figs. 8d-f), the results with the 4 different versions of CBS are indistinguishable from each other apart from during a few extreme rainfall events. When a CBS is used, in Cagliari or London, the fluctuations of *s* due to rain and evaporation have a lower amplitude than in the absence of a CBS. At points B and C, all the CBSs maintain high values of suction even during rainfall (Figs. 8b-c and 8e-f). At the toe of the slope (point A), in Cagliari (Fig. 8a) only the CBS having the F.L. made of silty sand and a thickness of t_{CBS} = 100cm was able to prevent suction drops (i.e. breakthrough) at all times whereas in London (Fig. 8d) both CBSs having a thickness of t_{CBS} = 100cm were able to prevent suction drops at all times.

Increasing the thickness of the F.L. from 60cm to 100cm has two different effects. Firstly, use of a thicker CBS reduces the evaporation of water from the underlying soil into the atmosphere (because this has to pass through the CBS), thereby leading to lower values of suction in the underlying soil in the middle and at the top of the slope, in particular for the Cagliari weather (see Fig. 8b and 8c). However, in these locations, the suction values are always high and variations of suction in this very high suction range do not affect significantly the stability of the slope. Hence, this detrimental effect of increased F.L. thickness is not of practical significance. Secondly, however, and of greater practical significance, the use of a thicker F.L. improves the effectiveness of the CBS at preventing or limiting water breakthrough into the underlying soil in the lower part of the slope, hence preventing the underlying soil from attaining very low values of suction in this region. This beneficial effect of increased

F.L. thickness is apparent from examination of the minimum values of suction attained in the underlying soil at the toe of the slope after the most severe rainfall events (see Figs. 8a and 8d) and on the reduced areas of underlying soil affected by the reduction in suction (see Fig. 7).

The silty sand is more effective than the fine sand as a material for the F.L. in Cagliari. By contrast, the use of fine sand is equally or more effective than the use of silty sand as a material for the F.L. in London. The reason for this difference between the results observed for the weathers of Cagliari and London is related to the two different working mechanisms of the CBSs made of fine sand and silty sand and how they interact with weather conditions, as clarified below.

Fig. 9 shows the absolute liquid velocity $|\boldsymbol{q}_l|$ and degree of saturation S_l profiles within the CBSs at the toe, middle and top sections (see Fig. 7 for the section locations), at the end of the most critical rainfall event in Cagliari. The direction of the liquid velocity is mainly orientated in a direction parallel to the interface between the F.L. and the C.L. Hence, the lateral water diversion of the CBS is proportional to the area under the liquid velocity profiles in the F.L. in Figs. 9a-c. From the comparison between the profiles obtained in the F.L. for the CBSs made of fine sand and those made of silty sand, two different working mechanisms can be identified. The finer layers made of fine sand are characterised by relatively low values of degree of saturation over most of their depth (the degree of saturation is high only in a thin region close to the interface with the C.L.) and relatively high downslope liquid velocity values in the thin layer at high degree of saturation, i.e. high lateral water diversion. By contrast, the finer layers made of silty sand are characterised by relatively high values of degree of saturation over their entire depth and low downslope liquid velocity values over their entire depth, i.e. high water storage but low lateral water diversion. This means that the key response of the CBSs having the F.L. made of fine sand is to divert rainwater laterally down the slope to the drain located at the toe. On the other hand, the key response of the CBSs having the F.L. made of silty sand is to store water in the F.L. and subsequently remove it by evaporation, as occurs for horizontal CBSs. For the CBSs having the finer layers made of fine sand, the values of degree of saturation and liquid velocity in the lower part of the F.L. significantly increase moving down the slope (i.e. from section c-c to section a-a), as a result of the increase of the amount of diverted water. By contrast, the increase in degree of saturation and liquid velocity from the top to the toe is less significant for the finer layers made of silty sand because the lateral water diversion plays a minor role. For the finer layer made of fine sand, using a higher thickness

does not lead to a significantly improved performance of the CBS because the upper part of the F.L. remains at low values of degree of saturation and contributes little to the lateral water diversion capacity of the CBS, as shown by the comparison between the profiles obtained for t_{CBS} = 60cm and t_{CBS} = 100cm. By contrast, increasing the thickness of the F.L. when this is made of silty sand leads to a significant improvement of the performance of the CBS because the upper part of the F.L. significantly contributes to the water storage capacity. Similar observations for the working mechanisms of the CBSs can be done for the London weather (not shown here).

Fig. 10 shows the various components of the water balance (rain, evaporation, runoff and net infiltration) at the top atmospheric boundary (at the middle section of the slope) in terms of cumulative water flows. Flows entering the model are positive whereas flows leaving the model are negative. Net infiltration is the difference between flows entering the system (rain) and flows leaving the system (runoff and evaporation). Both in Cagliari and in London, the amount of evaporation from the bare underlying soil is higher than that from the CBSs, as shown by Figs. 10b and 10f. These figures also show that the use of a CBS with the F.L. made of silty sand leads to higher amounts of evaporation than with the F.L. made of fine sand, because more water is stored close to the ground surface and hence available for evaporation. It is also noted that the amount of evaporation in London is slightly higher than that in Cagliari. Although in Cagliari the potential for evaporation is higher (drier and warmer weather), a lower amount of rainfall means that there is less water available for evaporation (stored close to the ground surface) compared to London. Very limited runoff occurs both in Cagliari and in London without the presence of a CBS and no runoff occurs in any of the models with a CBS (see Figs. 10c and 10g). As a result of the evaporation patterns described above, the CBS with the F.L. made of silty sand leads to a lower amount of net infiltration (see Figs. 10d and 10h) than a F.L. made of fine sand. In Cagliari, the cumulative net infiltration into the CBSs with the F.L. made of silty sand stabilise at approximately constant values in the long-term, suggesting that, in these cases, the CBSs rely almost entirely on the water storage capacity (no significant contribution of water transfer down the slope), because the amount of rain is approximately balanced by the amount of evaporation in the long term.

A high water storage capacity is generally useful in situations and climates in which the water storage capacity of the CBS is easily recharged so that it is fully available for the subsequent rainfall event, i.e. this is typical of warm and predominantly dry climatic conditions, with occasional intense rainfall. In cool

and persistently wet climates, in which the water storage capacity is often fully or partially occupied, a high lateral water diversion capacity is expected to be more useful as a means of dealing with periods of maximum rainfall intensity (Ross, 1990). In Cagliari, which is characterised by a relatively dry and warm weather, a CBS made of silty sand is likely to work better because a high amount of evaporation and a relatively low annual rainfall means that a large proportion of its high water storage capacity is typically available when an extreme rainfall event occurs. In London, which is characterised by cooler and more persistently wet weather, a CBS made of silty sand is probably less effective because the amount of evaporation is always much lower than the amount of rainfall, so much of the high water storage capacity is likely to be already filled even before an extreme rainfall event occurs. In London, where the extreme individual rainfall events are comparable or less extreme than the extreme rainfall events recorded in Cagliari, a CBS made of fine sand is likely to work better on a slope because it uses the high lateral water diversion capacity.

4.3 Effect of the use of multiple drains

CBSs working mainly by diverting water laterally down the slope (i.e. F.L. made of fine sand) may not be effective at preventing water breakthrough into the underlying soil when applied to tall slopes, due to limits in the water diversion length. A possible solution to this limitation is to use multiple drains placed in the CBS at intermediate heights.

The results of two simulations are compared in this section: the model with a single drain at the toe and the model with two drains, one at the toe and one at mid-height (see Fig. 2g). The models analysed are Cag_10_SCB_FS_60_SD and Cag_10_SCB_FS_60_MD. For both models, the slope height was H_s = 10m, the CBS was 60cm-thick, the F.L. was made of fine sand and the weather conditions of Cagliari were simulated.

Fig. 11 show the degree of saturation contours at the end of the most critical rainfall event for the two models. It can be seen that, unlike the single drain model in which a significant amount of water breakthrough into the underlying soil occurred at the toe, the multi-drain model was effective in preventing any water breakthrough into the underlying soil. All the water diverted by the CBS in the upper part of the slope was collected by the intermediate drain. Below this, the F.L. of the CBS was

again at low degree of saturation, suggesting that the lateral water diversion capacity was fully restored below the intermediate drain.

Fig. 12 shows the absolute liquid velocity and degree of saturation profiles in the CBS at the end of the most critical rainfall event at four different sections (see the locations of the sections in Fig. 11). Comparing the results obtained for the single drain and the multi-drain models, it can be seen that the profiles above the intermediate drain (section c-c in Figs. 12c,g and section d-d in Figs. 12d,h) were approximately coincident, meaning that the water was diverted laterally down the slope in the same way at these locations. Further down the slope than the intermediate drain (section a-a in Figs. 12a,e and section b-b in Figs. 12b,f), the models with a single drain and with multiple drains led to significantly different results. The degree of saturation and the absolute liquid velocity profiles obtained with a single drain attained much greater values than those attained with multiple drains. Indeed, unlike the model with a single drain, in the model with multiple drains all the lateral water diversion capacity was restored beneath the intermediate drain because the water transported from the upper part of the slope was collected into the intermediate drain. Therefore, the CBS can be seen as divided into two parts which work separately, one above and one below the intermediate drain.

The idea behind the use of multiple drains is to reduce the distance between the top of the slope, where the lateral water diversion starts, and the drain, where the water is collected, to make it lower than the maximum diversion length of the CBS. In other words, the intention is that in the CBS below an intermediate drain the ability of diverting water should be fully restored, because all the water transported from the section of slope above is collected by this intermediate drain. Theoretically, this concept can be extended to any number of drains and, thus, to slopes of any height. From a design point of view, a multi-drain CBS will be efficient in preventing water breakthrough if the following condition is verified:

$$\frac{L_{CBS}}{n_{drains}} \leq L_D \quad (4)$$

where L_{CBS} is the total length of the CBS measured in the horizontal direction, n_{drains} is the number of drains uniformly spaced and L_D is the diversion length of the CBS, which can be calculated using formulations from the literature (e.g. Ross, 1990; Parent and Cabral, 2006).

4.4 Effect of the use of multi-layered CBSs

An alternative method to extend the applicability of CBSs to higher slopes is the use of multi-layered CBSs. Scarfone (2020) developed an engineered approach to improve the water storage capacity of CBSs by means of the insertion of multiple intermediate coarser layers. The upper part of thick finer layers made of relatively coarse materials, such as fine sand, are typically at low degree of saturation (as shown in Fig. 9) and provides little contribution to the water storage capacity of the CBS. The insertion of intermediate coarser layers replicates the capillary barrier effect at the different interfaces between a F.L. (above the interface) and a C.L. (below the interface), leading to the possibility of a higher total water storage capacity by taking advantage of the high values of S_l achievable in the lower part of every finer layer. A similar approach based on the replication of the capillary barrier effect in multi-layered CBSs can be applied to the lateral water diversion of sloping CBSs (i.e. total diversion capacity can be increased by the possibility of high lateral water velocities down the slope in the lower part of every finer layer).

Two models are analysed in this section: a single CBS (SCB) and a multi-layered CBS (MCB) (see Fig. 2f). The models analysed are Cag_10_SCB_FS_60_SD and Cag_10_MCB_FS_60_SD. For both models, the slope height was H_s = 10m, the CBS was 60cm-thick with a single drain at the toe, the finer layers were made of fine sand and the weather conditions of Cagliari were simulated.

Fig. 13 show the degree of saturation contours at the end of the most critical rainfall event for the two models. It can be seen that, unlike the SCB, the MCB was effective in preventing any water breakthrough into the underlying soil. In the zoomed view in the upper part of the slope of Fig. 13b, it can be seen that the upper finer layer of the MCB attained high values of degree of saturation whereas the other three layers attained very low values of degree of saturation. At this location, all the rainwater was thus transported only by the upper finer layer. From the observation of the zoomed view at the toe, water breakthrough from the upper finer layer into the intermediate coarser layer, and then into the lower finer layer, occurred in the bottom few metres of the slope. The rainwater entering the lower finer layer was then diverted laterally down the slope by the lower finer layer. Just beyond the toe, where the CBS is horizontal, all the rainwater still transported by the upper finer layer broke through the underlying layers of the CBS and finally entered the drain. Similarly, the small amount of water diverted by the lower finer layer is directly collected by the drain located at the toe.

In order to understand the working principle of the MCB compared to the SCB, the absolute liquid velocity profiles and the degree of saturation profiles at the end of the most critical rainfall event in the two CBSs are compared in Fig. 14. Five different sections are considered in this figure, progressively from section A-A at the toe to section E-E at the top (see Fig. 13 for the section locations). In the single CBS, values of absolute liquid velocity (Fig. 14a) and degree of saturation (Fig. 14b) increased from the top of the slope (section E-E) in the down-dip direction until section B-B. Beyond B-B, the profiles in section A-A (toe) were approximately coincident with those obtained in section B-B, hence suggesting that at section B-B the water diversion capacity of the single CBS is reached and no further water can be diverted laterally down the slope. Hence, additional rainwater at that location resulted in water breakthrough. In the multi-layered CBS, moving from section E-E (top of the slope) down to section C-C, the absolute liquid velocity (Fig. 14c) and the degree of saturation (Fig. 14d) in the upper finer layer increased whereas no water is transported in the other layers. All the rainwater was thus diverted by the upper finer layer between sections E-E and C-C. At sections B-B and A-A, the profiles in the upper finer layer remained similar to those obtained in section C-C suggesting that at section B-B the upper finer layer reached the diversion capacity and could not divert any extra water. Therefore, from section B-B downwards, all extra rainwater broke through into the intermediate coarser layer and then into the lower finer layer. From section B-B to section A-A, the degree of saturation in the lower finer layer increased as well as the absolute liquid velocity. Therefore, between section B-B and section A-A the lower finer layer started diverting rainwater laterally in addition to the upper finer layer.

Therefore, the functioning of this sloping multi-layered CBS can be seen schematically as follows:

- at the top of the slope rainwater is diverted laterally down the slope by the upper finer layer;
- when the diversion capacity of the upper F.L. is attained, breakthrough into the underlying coarser layer and then into the lower finer layer occurs;
- from this point, in addition to the upper finer layer which keeps diverting an amount of water equal to the diversion capacity, the lower finer layer starts diverting water;
- this mechanism is expected to be replicable for multiple layers.

According to this mechanism, the diversion capacity of the MCB analysed in this section is expected to be approximately twice that of the SCB.

4.5 Assessment of the slope stability

The slope stability was assessed for the different models previously presented at various critical rainfall events, by means of the limit analysis software LimitState:GEO. The models with no CBS were first analysed to assess the stability of the bare slopes (BS). Subsequently, the models with CBSs were analysed to assess the effect of the CBSs on slope stability. In particular, for each FE model including a CBS, two LA models were analysed:

i) the whole system which was the slope covered by a CBS (CS), hence made of the CBS plus the underlying soil (CS-CBS+U.S.), in which the overall stability was assessed;

ii) the slope covered by a CBS (CS), in which only the stability of the underlying soil is assessed (CS-U.S.).

In other words, the same distribution of the product $s \cdot S_l$ (from Code_Bright) was used in these two models but in the latter model the CBS was not modelled in LS:GEO and only the stability of the underlying soil was assessed.

The results are presented in terms of Factor of Safety (FoS). Considering that the shear strength was modelled by Equation 1, the FoS is here defined as:

$$FoS = \frac{\tan \phi'}{\tan \phi_{lim}} = \frac{c'}{c_{lim}} \quad (5)$$

where ϕ_{lim} and c_{lim} are respectively the limit friction angle and the limit effective cohesion which together would cause failure (i.e. for FoS=1). Note that FoS is therefore a scaling factor which acts simultaneously on ϕ' and c'.

Fig. 15 shows the failure mechanisms and the corresponding minimum factors of safety at the most critical rainfall event in Cagliari for a slope height of H_s = 10m. Figs. 15b and 14c refer to the model with the CBS having the F.L. made of fine sand and a thickness of t_{CBS} = 60cm. The BS model had a shallow failure line passing though the fully saturated area (Fig. 15a). The corresponding FoS was lower than 1, i.e. FoS=0.82, suggesting that, without a CBS, the slope was unstable at the end of the most critical rainfall event. The use of a CBS significantly improved the stability of the original soil, as shown by the CS–U.S. model (Fig. 15c), thanks to the higher suction values maintained in the underlying soil. The failure line was much deeper and the corresponding FoS was much higher than 1 (FoS=52). For the CS-CBS+U.S. model, the stability of the CBS became more critical than that of the U.S. The failure mechanism of the model CS–CBS+U.S. involved only the C.L. and the F.L. of the CBS but the

corresponding FoS was higher than 1 (FoS=1.29) which corresponded to a stable condition. Similar failure mechanisms were observed for the other models.

Fig. 16a shows the time history of the minimum FoS of the three models discussed above at various critical rainfall events. The minimum FoS represents the most critical failure surface for each model. In Cagliari, in two events the FoS of the BS was lower than 1. Introducing the CBS, the underlying soil was permanently stable with corresponding FoS values always very high, above 40. For comparison, Fig. 16b shows the time history of the FoS for the same three models but subjected to the weather conditions of London. In this case, the FoS of the BS was lower than 1 for most critical rainfall events. Introducing the CBS, the underlying soil was permanently stable with corresponding FoS values between 1.3 and 1.6. In both Cagliari and London, the stability of the CBS was almost unaffected by the weather conditions, indicated by an approximately constant trend of the FoS, always higher than 1. This stable trend was related to the fact that the suction values attained in the materials used for a CBS, which are generally coarse-grained soils, are typically relatively low. The stability of the CBS is thus hardly affected by variations in suction and hence weather conditions. For these materials, the stability is mainly related to the shear strength parameters, i.e. ϕ' and c', and the value of ϕ' is often high for this type of materials. These shear strength parameters of the CBS materials are affected by fewer uncertainties and by minor variability compared to the impact of suction on the shear strength of the underlying soil. The prediction of the minimum values of suction attained in the underlying soil is often the result of predictive methods characterised by a higher number of uncertainties compared to laboratory and field tests used to characterise the shear strength parameters of the CBS materials.

Fig. 17 shows the minimum factors of safety obtained for all the models analysed (the FoS values relative to the CS-U.S. models are not shown in this graph). It can be seen that all the models with no CBS had a minimum FoS lower than 1. In particular, the slope height had a negligible effect on the minimum FoS of the models with no CBS in Cagliari. The FoS for the model in London was slightly lower, as a result of the lower suction values attained. All the models with a CBS led to a minimum FoS higher than 1, meaning that all the CBSs analysed were effective in guaranteeing the stability of the slopes in the long-term, even under extreme rainfall conditions. For all these models, the minimum FoS values were related to the stability of the CBSs.

All the models with CBSs made of fine sand led to similar values of the minimum FoS, approximately equal to 1.3, regardless of the thickness of the CBS, weather conditions, the use of multiple drains or the use of a multi-layered CBS. As noted above, in materials such as fine sand, suction plays a minor role in the shear strength, and hence changes of CBS design or weather conditions have relatively little impact on the FoS. The models with the F.L. made of silty sand showed slightly higher sensitivity of the minimum FoS to the thickness of the CBS due to the higher range of suction values attained by a material such as silty sand. At the end of the most critical rainfall event, the CBS with silty sand and t_{CBS} = 60cm experienced lower values of suction than the CBS with silty sand and t_{CBS} = 100cm, in both Cagliari and London (see Figs. 7d, 7e, 7i and 7j). For the CBSs with t_{CBS} = 60cm, the factor of safety is lower when silty sand is used for the F.L. than when fine sand is used, because the friction angle of the silty sand (ϕ' = 35°) is less than the friction angle of the fine sand (ϕ' = 40°).

It must be noted that the small amount of water breakthrough into the underlying soil that occurred in some models did not affect significantly the stability of the slope because the critical failure surface did not pass through the area affected by water breakthrough. In other words, some small amount of water breakthrough into the underlying soil can be accepted without compromising the stability of the slope.

5. Conclusions

The application of Capillary Barrier Systems for suction control and prevention of rainfall-induced slope instability was studied numerically in this paper by means of advanced 2D thermo-hydraulic FE analyses and limit analyses. Various models were analysed in order to assess the role of different variables in the problem, such as the slope height, thickness and materials of the CBS, weather conditions and alternative solutions like the use of multiple drains and multi-layered CBSs.

Sloping CBSs may find application for slopes made of relatively weak materials, which are at risk of rainfall-induced slope instability. CBSs will be potentially useful if the slope angle is within an appropriate range (between the friction angle of the underlying soil and the friction angle of the materials of the CBS). For very low slope angles the slope would be stable without a CBS, whereas for very high slope angles the CBS itself would be unstable.

From the analyses, it was found that all the CBSs were in general effective at preventing or limiting the percolation of water into the underlying soil, to maintain high values of suction in the underlying soil and to maintain the stability of the slope even during intense rainfall events, for the different weather conditions analysed. It was shown that a small amount of water breakthrough into the underlying soil can be tolerated without affecting the slope stability, as long as this breakthrough affects only a small area of underlying soil and the potential failure mechanisms do not involve this area.

Depending upon the material used for the finer layer, two key working principles of sloping CBSs were identified. Using a finer material for the finer layer, such as a silty sand, the lateral water diversion ability of the CBS is limited and the behaviour is hence similar to that of a horizontal CBS, i.e. rainwater is stored in the finer layer and released into the atmosphere by evaporation. This type of CBS is more effective if applied in regions with a warm and predominantly dry climate, with occasional intense rainfall events, where the amounts of evaporation and rain are comparable. For this type of CBS, using a thick finer layer is typically beneficial because this increases the water storage capacity. The use of a finer material for the finer layer of the CBS is also likely to lead to a higher amount of evaporation, because more water is stored close to the ground surface and hence is available for evaporation. Using a slightly coarser material for the finer layer, such as a fine sand, rainwater entering the finer layer is diverted laterally down the slope into a drain due to the effect of gravity. The effectiveness of this type of CBS is little affected by the overall climatic conditions but it strongly depends on the intensity of extreme rainfall events. For this type of CBS, using a thicker finer layer does not improve significantly the water diversion capacity because most of the water is diverted within a thin sub-layer of the finer layer, immediately above the interface with the coarser layer.

The effectiveness of CBSs at preventing water breakthrough decreases with increasing slope height, in particular for CBSs whose main working principle is lateral water diversion. For this reason, two solutions aimed to widen the range of applicability of CBSs to higher slopes were analysed and discussed: the use of multi-layered CBSs and/or multiple drains. In multi-layered CBSs, the capillary barrier effect is replicated at multiple interfaces between a F.L. (above the interface) and a C.L. (below the interface). In this way, the lateral water diversion ability is replicated within almost the whole thickness of the CBS whereas for a single CBS made of a relatively coarse F.L. this would be limited to a sub-layer at the bottom of the F.L. Scarfone (2020) showed that, if designed appropriately, multi-

layered CBSs also have greater storage capacity than conventional CBSs, meaning that, when used on slopes, they will exhibit better performance than conventional CBSs even when water storage is the main working mechanism. Sloping CBSs employing water diversion as the main working mechanism can be applied to slopes of any height if multiple drains are placed across the slope at different locations down the slope. In this way, the water diversion capacity of the CBS is fully restored below each intermediate drain, which therefore collects only the water diverted by the part of the CBS on the section of slope up to the next drain.

All the tested CBSs under both Cagliari and London weather conditions were effective at stabilizing the slopes. After the application of CBSs, the problem of the stability was controlled by the stability of the CBS (i.e. the critical slip surface was entirely within the CBS). This is highly desirable, because a CBS is typically made of relatively coarse-grained materials, having good mechanical properties and shear strength little affected by variability of suction, and thus weather conditions, which are affected by more uncertainties. In addition, the friction angle of the materials used for the CBS can be controlled during construction because it strongly depends on the degree of compaction and void ratio.

The numerical modelling approach described in this paper has been fully validated against experimental results only for the limited case of 1-D conditions (i.e. horizontal CBSs). Hence, the conclusions of the parametric study of sloping CBSs presented in this paper still require appropriate experimental validation. This is likely to be a major research undertaking, involving substantial field studies with more detailed material characterisation and long-term monitoring of appropriate variables than has previously been achieved, as it can only be done at full scale.

References

Abdolahzadeh AM, Lacroix Vachon B and Cabral AR. Evaluation of the effectiveness of a cover with capillary barrier effect to control percolation into a waste disposal facility. *Canadian Geotechnical Journal*, 48(7):996–1009.

Baker RS and Hillel D (1990). Laboratory tests of a theory of fingering during infiltration into layered soils. *Soil Science Society of America Journal*, 54(1):20–30.

Bishop AW (1959). The principle of effective stress. *Teknisk ukeblad*, 39, 859-863.

Brutsaert W (1982). *Evaporation into the atmosphere: Theory, history and applications* (D. Reidel).

Dwyer SF (1998). Alternaltive landfill covers pass the test. *Civil engineering*, 68(9):50.

Gallipoli D, Gens A, Chen G and D'Onza F (2008). Modelling unsaturated soil behaviour during normal consolidation and at critical state. *Computers and Geotechnics*, 35(6):825–834.

Harnas FR, Rahardjo H, Leong EC and Wang JY (2014). Experimental study on dual capillary barrier using recycled asphalt pavement materials. *Canadian Geotechnical Journal*, 51(10):1165–1177.

Harnas FR, Rahardjo H, Leong EC and Wang JY (2016). Physical model for the investigation of capillary-barrier performance made using recycled asphalt. *Geotechnical Testing Journal*, 39(6):977–990.

Henken-Mellies WU and Schweizer A (2011). Long-term performance of landfill covers results of lysimeter test fields in Bavaria (Germany). *Waste Management & Research*, 29(1):59–68.

Iverson RM (2000). Landslide triggering by rain infiltration. *Water resources research*, 36(7), 1897-1910.

Kämpf M and Montenegro H (1997). On the performance of capillary barriers as landfill cover. *Hydrology and Earth System Sciences*, 1(4):925–930.

Khire MV, Benson CH and Bosscher PJ (2000). Capillary barriers: Design variables and water balance. *Journal of Geotechnical and Geoenvironmental Engineering*, 126(8):695–708.

Lacroix Vachon B, Abdolahzadeh AM and Cabral AR (2015). Predicting the diversion length of capillary barriers using steady state and transient state numerical modeling: case study of the Saint-Tite-des-Caps landfill final cover. *Canadian Geotechnical Journal*, 52(12):2141–2148.

LimitState (2019). *LimitState:GEO Manual VERSION 3.5.d, March 2019 edn*. LimitState Ltd.

Morris CE and Stormont JC (1998). Evaluation of numerical simulations of capillary barrier field tests. *Geotechnical & Geological Engineering*, 16(3):201–213.

Morris CE and Stormont JC (1999). Parametric study of unsaturated drainage layers in a capillary barrier. *Journal of Geotechnical and Geoenvironmental Engineering*, 125(12):1057–1065.

Mualem Y (1976). A new model for predicting the hydraulic conductivity of unsaturated porous media. *Water Resources Research*, 12(3):513–522.

Ng CWW, Coo JL, Chen ZK and Chen R (2016). Water infiltration into a new three layer landfill cover system. *Journal of Environmental Engineering*, 142(5):04016007.

Ng CWW, Liu J, Chen R and Xu J (2015). Physical and numerical modeling of an inclined three-layer (silt/gravelly sand/clay) capillary barrier cover system under extreme rainfall. *Waste Management*, 38:210–221.

Ng CWW and Shi Q (1998). A numerical investigation of the stability of unsaturated soil slopes subjected to transient seepage. *Computers and Geotechnics*, 22(1), 1-28.

Oldenburg CM and Pruess K (1993). On numerical modeling of capillary barriers. *Water Resources Research*, 29(4):1045–1056.

Olivella S, Gens A, Carrera J and Alonso EE (1996). Numerical formulation for a simulator (CODE_BRIGHT) for the coupled analysis of saline media. *Engineering computations*, 13(7):87–112.

Olivella S, Vaunat J and Rodriguez-Dono A (2021). Code_Bright 2021 User's Guide. Accessible at: https://deca.upc.edu/en/projects/code_bright.

Parent SÉ and Cabral A (2006). Design of inclined covers with capillary barrier effect. *Geotechnical & Geological Engineering*, 24(3):689–710.

Pease RE and Stormont JC (1996). Effectiveness of sloping capillary barriers under high precipitation rates. In *Joint Conference on the Environment*.

Polemio M and Petrucci O (2000). Rainfall as a landslide triggering factor an overview of recent international research. *Landslides in Research, Theory and Practice: Proceedings of the 8th International Symposium on Landslides held in Cardiff on 26–30 June 2000*.

Rahardjo H, Santoso VA, Leong EC, Ng YS and Hua CJ (2011). Performance of an instrumented slope covered by a capillary barrier system. *Journal of Geotechnical and Geoenvironmental Engineering*, 138(4):481–490.

Rahardjo H, Santoso VA, Leong EC, Ng YS, Tam CPH and Satyanaga A (2013). Use of recycled crushed concrete and Secudrain in capillary barriers for slope stabilization. *Canadian Geotechnical Journal*, 50(6):662–673.

Rahardjo H, Satyanaga A, Harnas F and Leong EC (2016). Use of dual capillary barrier as cover system for a sanitary landfill in Singapore. *Indian Geotechnical Journal*, 46(3):228–238.

Rahardjo H, Satyanaga A and Leong EC (2007). Characteristics of pore-water pressure response in slopes during rainfall. In *Proceedings of 3rd Asian Conference on Unsaturated Soils*, pages 493–498.

Rahardjo H, Satyanaga A and Leong EC (2011). Unsaturated soil mechanics for slope stabilization. In *Proceedings of 5th Asia–Pacific conference on unsaturated soils*, page 103–117.

Ross B (1990). The diversion capacity of capillary barriers. *Water Resources Research*, 26(10):2625–2629.

Scarfone R (2020). Modelling the hydraulic behaviour of unsaturated soils and application to the numerical and experimental study of capillary barrier systems. PhD thesis, University of Glasgow.

Scarfone R, Wheeler SJ and Lloret-Cabot M (2020a). Conceptual hydraulic conductivity model for unsaturated soils at low degree of saturation and its application to the study of capillary barrier systems. *Journal of Geotechnical and Geoenvironmental Engineering*, *146*(10), 04020106.

Scarfone R, Wheeler SJ and Lloret-Cabot M (2020b). A hysteretic hydraulic constitutive model for unsaturated soils and application to capillary barrier systems. *Geomechanics for Energy and the Environment*, 100224.

Smith CC and Gilbert M (2007). Application of discontinuity layout optimization to plane plasticity problems. *Proceedings of the Royal Society A: Mathematical, Physical and Engineering Sciences*, 463(2086):2461–2484.

Steenhuis TS, Parlange J-Y and Kung K-JS (1991). Comment on "The diversion capacity of capillary barriers" by Benjamin Ross. *Water Resources Research*, 27(8):2155–2156.

Stormont JC (1995). The effect of constant anisotropy on capillary barrier performance. *Water Resources Research*, 31(3):783–785.

Stormont J (1996). The effectiveness of two capillary barriers on a 10% slope. *Geotechnical & Geological Engineering*, 14(4):243–267.

Stormont JC and Anderson CE (1999). Capillary barrier effect from underlying coarser soil layer. *Journal of Geotechnical and Geoenvironmental Engineering*, *125*(8), 641-648.

Stormont JC and Morris CE (1997). Unsaturated drainage layers for diversion of infiltrating water. *Journal of irrigation and drainage engineering*, 123(5):364–366.

Stormont JC and Morris CE (1998). Method to estimate water storage capacity of capillary barriers. *Journal of Geotechnical and Geoenvironmental Engineering*, 124(4):297–302.

Suter GW, Luxmoore RJ and Smith ED (1993). Compacted soil barriers at abandoned landfill sites are likely to fail in the long term. *Journal of Environmental Quality*, 22(2):217–226.

Swiss Standard SN 670 010b (1999). Characteristic coefficients of soils, association of Swiss road and traffic engineers.

van Genuchten MT (1980). A closed-form equation for predicting the hydraulic conductivity of unsaturated soils 1. *Soil science society of America journal*, 44(5): 892-898.

Webb SW (1997). Generalization of Ross' tilted capillary barrier diversion formula for different two-phase characteristic curves. *Water Resources Research*, 33(8):1855–1859.

Yang H, Rahardjo H and Leong E-C (2006). Behavior of unsaturated layered soil columns during infiltration. *Journal of Hydrologic Engineering*, 11(4):329–337.

Yang H, Rahardjo H, Leong E-C and Fredlund DG (2004a). A study of infiltration on three sand capillary barriers. *Canadian Geotechnical Journal*, 41(4):629–643.

Yang H, Rahardjo H, Wibawa B and Leong EC (2004b). A soil column apparatus for laboratory infiltration study. *Geotechnical Testing Journal*, 27(4):347–355.

Zhan TLT, Li H, Jia GW, Chen YM and Fredlund DG (2014). Physical and numerical study of lateral diversion by three-layer inclined capillary barrier covers under humid climatic conditions. *Canadian Geotechnical Journal*, 51(12):1438–1448.

Zhang ZF (2016). Evaluating the long-term hydrology of an evapotranspiration-capillary barrier with a 1000 year design life. *Water Resources Research*, 52(6):4883–4904.

Zhang W, Sun C and Qiu Q (2016). Characterizing of a capillary barrier evapotranspirative cover under high precipitation conditions. *Environmental Earth Sciences*

Table 1. Constitutive laws and parameters used in the FE analyses

Soil water retention curve, SWRC (Scarfone et al, 2020a)	$S_{le,d} = \left\{1+\left[\frac{\left(s^{\gamma_d} - A_d\right)^{1/\gamma_d}}{P_{0d}}\right]^{n_d}\right\}^{-m_d}$ $S_{le,w} = \left\{1+\left[\frac{\left(s^{-\gamma_w} - A_w\right)^{-1/\gamma_w}}{P_{0w}}\right]^{n_w}\right\}^{-m_w}$ $S_{l,d} = \xi_d \ln\left(\frac{S_{dry}}{s}\right) + \left[S_{ls,d} - \xi_d \ln\left(\frac{S_{dry}}{s}\right)\right] \cdot S_{le,d}$ $S_{l,w} = \xi_w \ln\left(\frac{S_{dry}}{s}\right) + \left[S_{ls,w} - \xi_w \ln\left(\frac{S_{dry}}{s}\right)\right] \cdot S_{le,w}$	**Fine sand**	P_{0d}=2.31E-3 MPa, P_{0w}=1.21E-3 MPa, m_d=m_w=0.779, ξ_d=ξ_w=6.79E-3, S_{lsd}=S_{lsw}=1, γ_d=γ_w=8, s_{dry}=1 GPa
		Silty sand	P_{0d}=1.16E-2 MPa, P_{0w}=6.05E-3 MPa, m_d=m_w=0.779, ξ_d=ξ_w=1.36E-2, S_{lsd}=S_{lsw}=1, γ_d=γ_w=8, s_{dry}=1 GPa
		Gravelly sand	P_{0d}=1.93E-4 MPa, P_{0w}=6.45E-4 MPa, m_d=m_w=0.688, ξ_d=ξ_w=3.27E-3, S_{lsd}=S_{lsw}=1, γ_d=γ_w=6, s_{dry}=1 GPa
		Silt	P_{0d}=1.12E-1 MPa, P_{0w}=2.52E-2 MPa, m_d=m_w=0.186, ξ_d=ξ_w=0, S_{lsd}=S_{lsw}=1, γ_d=γ_w=2
Soil hydraulic conductivity curve, SHCC (Scarfone et al, 2020b)	$k_l = k_{ls} \cdot \sqrt{S_l^C}\left[1-\left(1-\left(S_l^B\right)^{1/m}\right)^m\right]^2 + C^{Film} \cdot \left(a^{Film} + s\right)^{-1.5}$ $S_l^C = \frac{S_l - S_{l,BWC/BWD}}{S_{ls} - S_{l,BWC/BWD}}$ $S_l^B = \frac{S_l - S_{l,BWE/BWEX}}{S_{ls} - S_{l,BWE/BWEX}}$	**Fine sand**	k_{ls}=2.70E-4 m/s, $S_{l,BWC}$=$S_{l,BWD}$=$S_{l,BWE}$=$S_{l,BWEX}$=0.18, a^{Film}=4E-5 MPa, C^{Film}=2.575E-13 MPa$^{1.5}$ms^{-1}
		Silty sand	k_{ls}=1.08E-5 m/s, $S_{l,BWC}$=$S_{l,BWD}$=$S_{l,BWE}$=$S_{l,BWEX}$=0.22, a^{Film}=2E-4 MPa, C^{Film}=1.287E-12 MPa$^{1.5}$ms^{-1}
		Gravelly sand	k_{ls}=7.60E-2 m/s, $S_{l,BWC}$=$S_{l,BWD}$=$S_{l,BWE}$=$S_{l,BWEX}$=0.16, a^{Film}=1.45E-7 MPa, C^{Film}=1.682E-14 MPa$^{1.5}$ms^{-1}
		Silt	k_{ls}=3.70E-7 m/s, $S_{l,BWC}$=$S_{l,BWD}$=$S_{l,BWE}$=$S_{l,BWEX}$=0.00, C^{Film}=0
Diffusion of water vapour in the gas phase - Fick's Law (Olivella et al, 2021)	$\mathbf{i}_g^{\mathbf{w}} = -\left(\tau\phi\rho_g S_g D_g^w \mathbf{I}\right)\nabla\omega_g^w$ $D_g^w = D\left[\frac{\left(273.15\text{K} + T\right)^n}{p_g}\right]$	**Fine sand**	ϕ=0.411, τ=1, D=5.9E-6 m^{2}Pas^{-1}K^{-n}, n=2.3
		Silty sand	ϕ=0.411, τ=1, D=5.9E-6 m^{2}Pas^{-1}K^{-n}, n=2.3
		Gravelly sand	ϕ=0.382, τ=1, D=5.9E-6 m^{2}Pas^{-1}K^{-n}, n=2.3
		Silty sand	ϕ=0.480, τ=1, D=5.9E-6 m^{2}Pas^{-1}K^{-n}, n=2.3
Conductive flux of heat - Fourier's Law (Olivella et al, 2021)	$\mathbf{i}_c = -\lambda\nabla T$ $\lambda = \lambda_{sat}\sqrt{S_l} + \lambda_{dry}\left(1-\sqrt{S_l}\right)$ $\lambda_{dry} = {\lambda_{solid}}^{(1-\phi)}{\lambda_{gas}}^{\phi}$, $\lambda_{sat} = {\lambda_{solid}}^{(1-\phi)}{\lambda_{liq}}^{\phi}$	**All materials**	λ_{solid}=7.7 Wm^{-1}K^{-1}, λ_{gas}=0.02619 Wm^{-1}K^{-1}, λ_{liquid}=0.591 Wm^{-1}K^{-1}

SWRC (subscript d for drying paths, subscript w for wetting paths): S_l=(liquid) degree of satuation; S_{le}=effective (liquid) degree of saturation; m, n, P_0 [MPa], γ=parameters controlling the shape of the SWRC, with n=1/(1-m); ξ: parameter controlling the residual degree of saturation function; s_{dry} [MPa]=suction corresponding to complete dryness; A=function of the last reversal point, controls the position of the scanning curve (A=0 for main wetting or main drying curves). **SHCC**: k_{ls}=saturated hydraulic conductivity; C^{film} [ms^{-1}MPa$^{1.5}$], a^{film} [MPa]= parameters governing the liquid film component of the hydraulic conductivity; $S_{l,BWD}$= bulk water discontinuity value of the degree of saturation; $S_{l,BWEX}$= bulk water exclusion value of the degree of saturation; $S_{l,BWC}$= bulk water continuity value of the degree of saturation; $S_{l,BWE}$= bulk water entry value of the degree of saturation. **Fick's Law**: $\mathbf{i}^{\mathbf{w}}_{\mathbf{g}}$ [kg m^{-3} s^{-1}]=diffusive water flow in the gas phase; τ=tortuosity; ϕ=porosity; ρ_g [kg/m^3]=gas density; S_g=gas degree of saturation (S_g=1-S_l); $D^w{}_g$ [m^2/s]=diffusion coefficient of water in the gas phase; $\omega^w{}_g$ [kg of water per kg of gas]=water mass fraction in the gas phase; D [m^2/s], n =parameters of the model; T [K]=temperature. **Fourier's Law**: $\mathbf{i}_c$ [W/m^2]=conductive heat flux; λ [W m^{-1} K^{-1}]=thermal conductivity; λ_{solid} [W m^{-1} K^{-1}]=thermal conductivity of the solid phase; λ_{gas} [W m^{-1} K^{-1}]=thermal conductivity of the gas phase; λ_{liq} [W m^{-1} K^{-1}]=thermal conductivity of the liquid phase.

Table 2. Parameters used in the Limit Analyses

Material	γ [kN/m^3]	ϕ' [°]	c' [kPa]
Fine sand	17	40	0.1
Silty sand	19	35	0.1
Gravelly sand	16	40	0.1
Silt	19	20	0.1

Table 3. Summary of the analyses

Analysis ID	Weather	H_s [m]	CBS			Drain
			type	material F.L.	t_{CBS} [cm]	
Cag_10_NOCBS	Cagliari	10		No CBS		-
Cag_10_SCB_FS_60_SD	Cagliari	10	Single	Fine sand	60	Single
Cag_10_SCB_FS_100_SD	Cagliari	10	Single	Fine sand	100	Single
Cag_10_SCB_SS_60_SD	Cagliari	10	Single	Silty sand	60	Single
Cag_10_SCB_SS_100_SD	Cagliari	10	Single	Silty sand	100	Single
Lon_10_NOCBS	London	10		No CBS		-
Lon_10_SCB_FS_60_SD	London	10	Single	Fine sand	60	Single
Lon_10_SCB_FS_100_SD	London	10	Single	Fine sand	100	Single
Lon_10_SCB_SS_60_SD	London	10	Single	Silty sand	60	Single
Lon_10_SCB_SS_100_SD	London	10	Single	Silty sand	100	Single
Cag_6_NOCBS	Cagliari	6		No CBS		-
Cag_6_SCB_FS_60_SD	Cagliari	6	Single	Fine sand	60	Single
Cag_10_SCB_FS_60_MD	Cagliari	10	Single	Fine sand	60	Multiple
Cag_10_MCB_FS_60_SD	Cagliari	10	Layered	Fine sand	60	Single

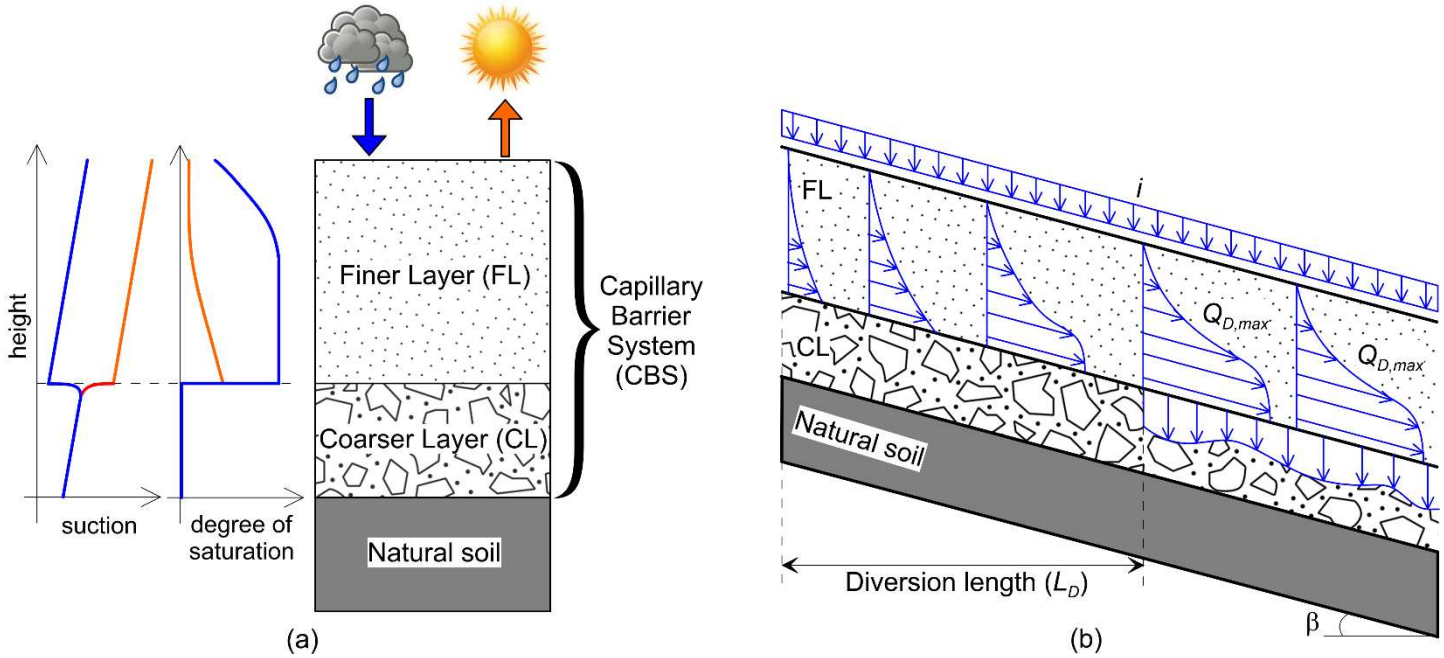

Fig. 1. Working mechanisms of (a) horizontal CBSs and (b) sloping CBSs.

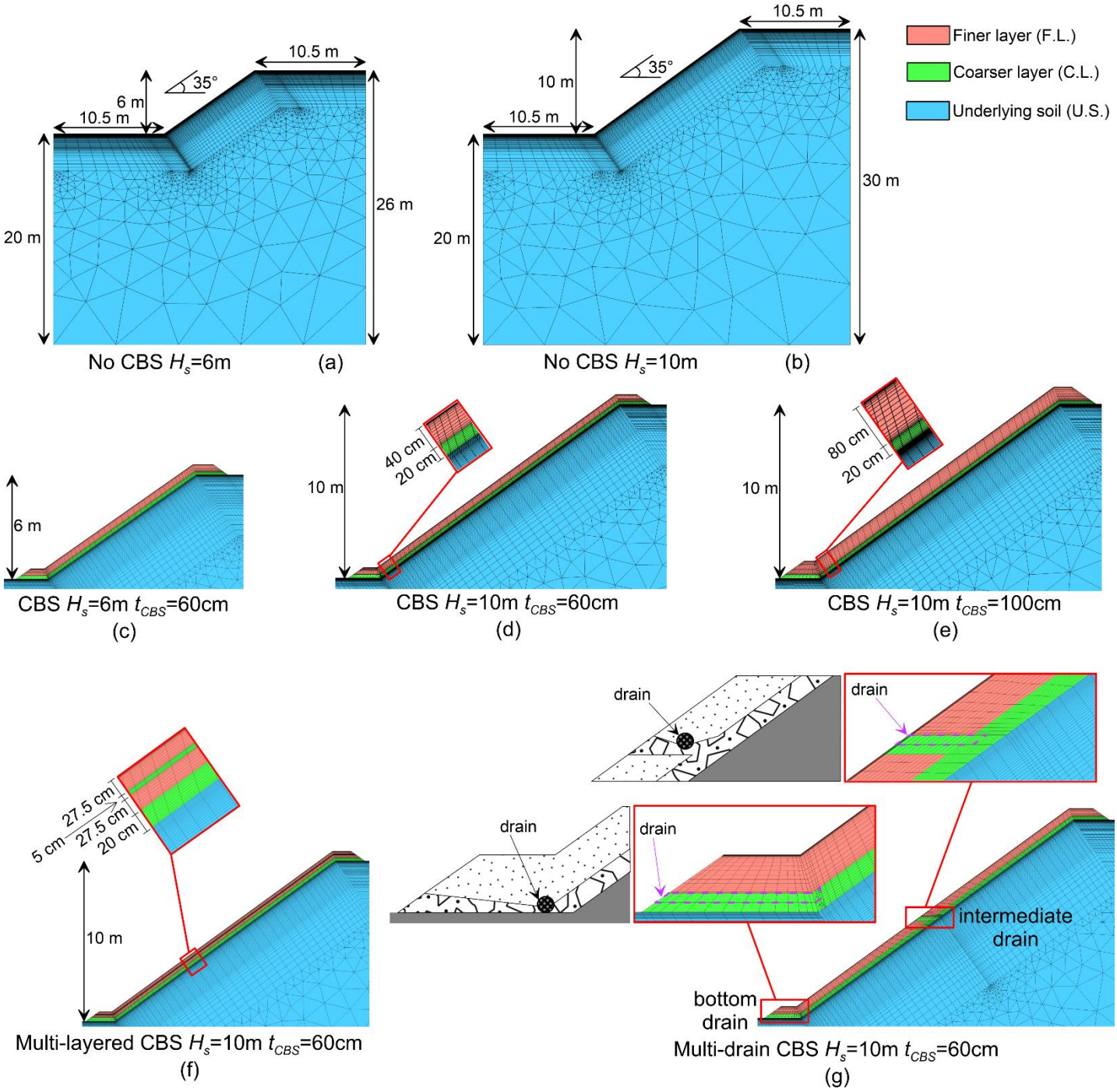

Fig. 2. Numerical models analysed.

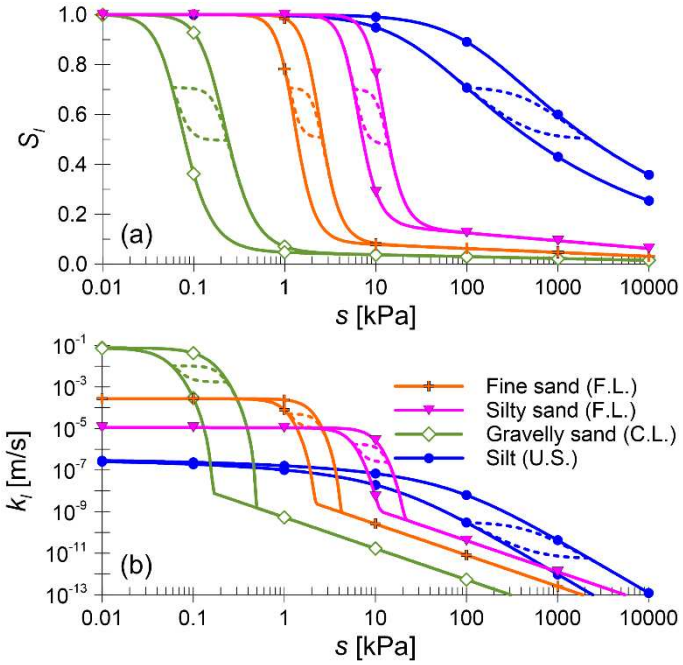

Fig. 3. Hydraulic properties of the materials: (a) SWRC and (b) SHCC.

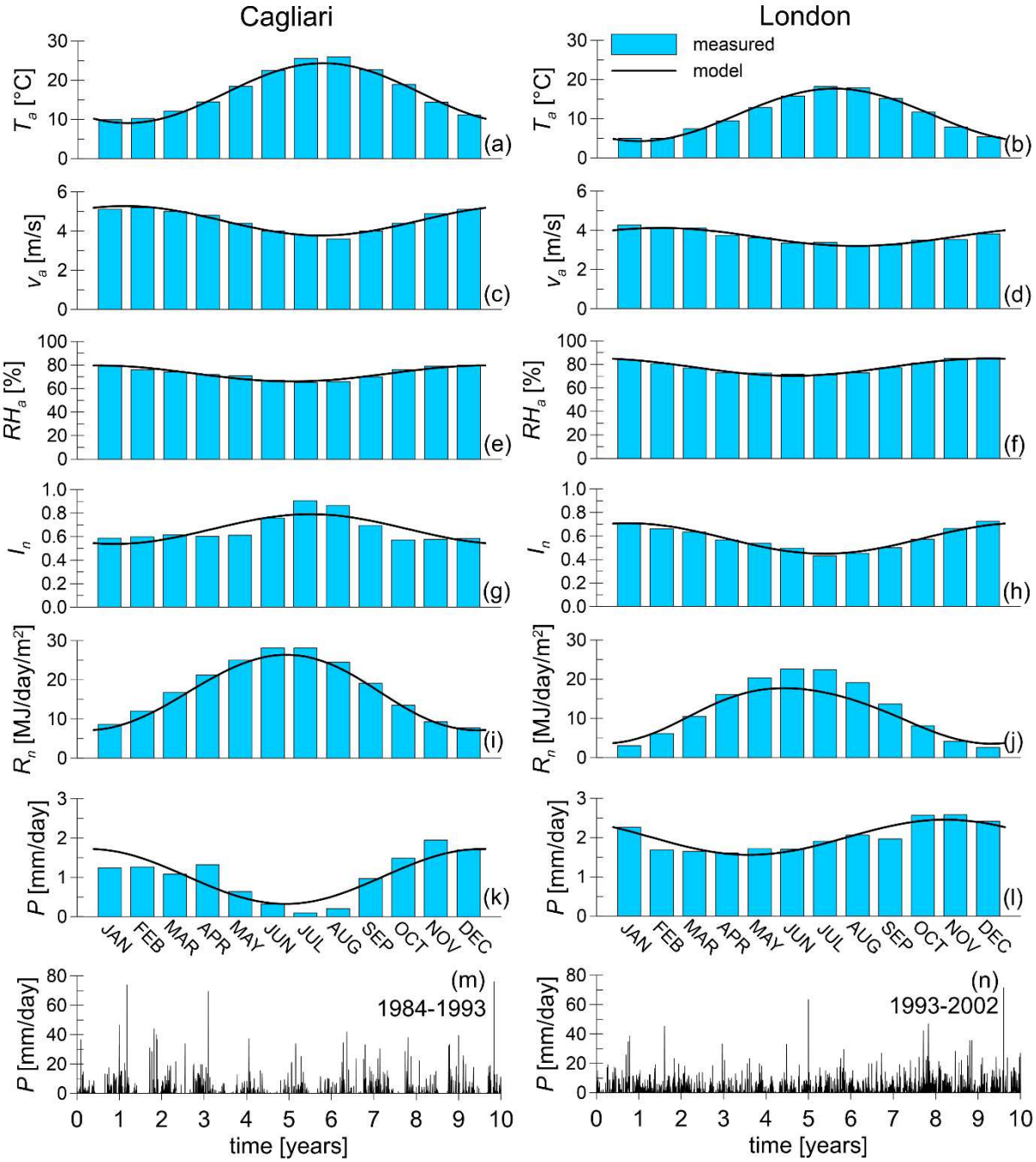

Fig. 4. Measured data and modelling of atmospheric conditions for (a,c,e,g,i,k,m) Cagliari (Italy) and (b,d,f,h,j,l,n) London (UK).

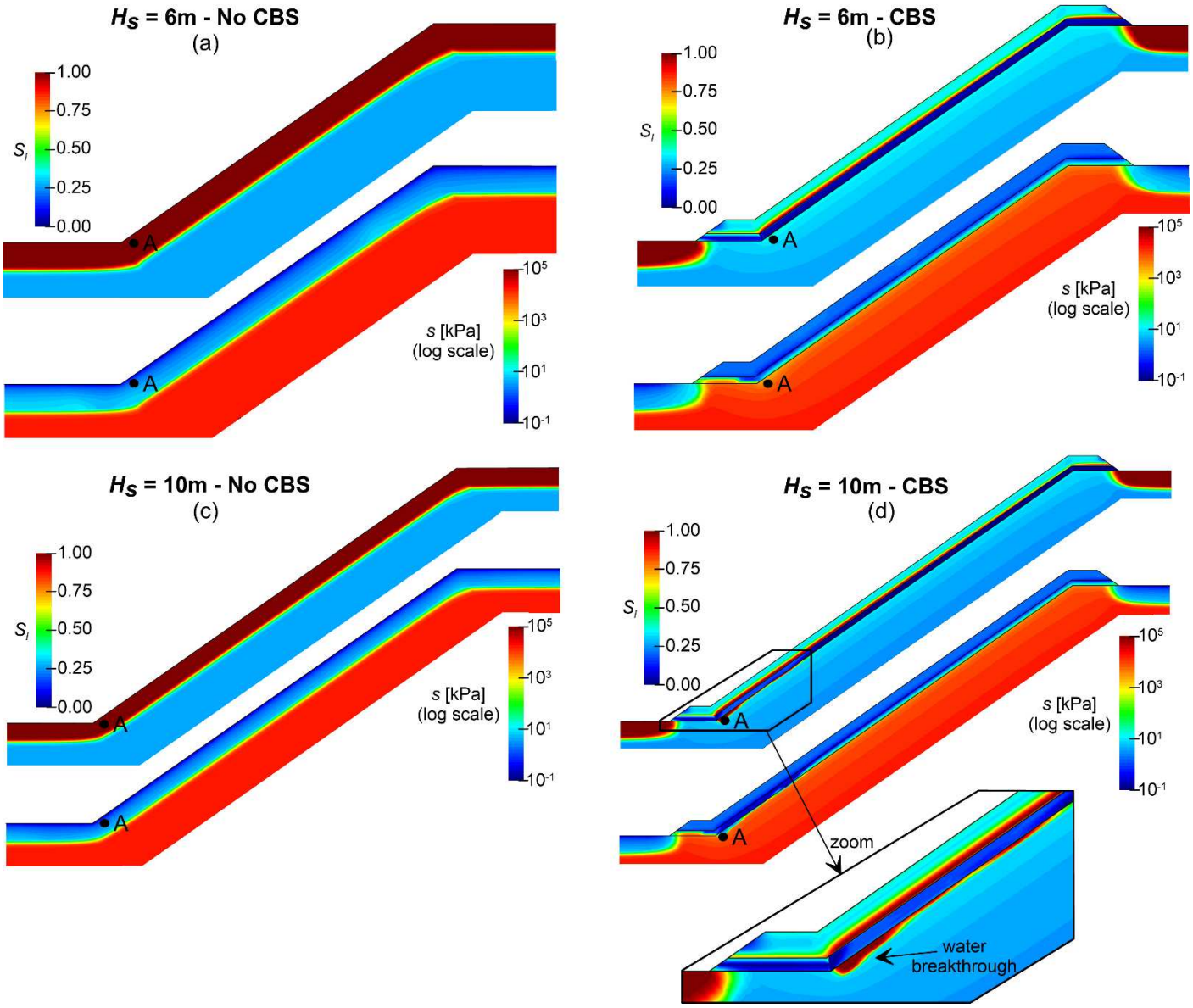

Fig. 5. Degree of saturation and suction contours at the most critical rainfall event in Cagliari, i.e. t =1.18274 years, for different slope heights: (a-b) H_s = 6m, (c-d) H_s = 10m.

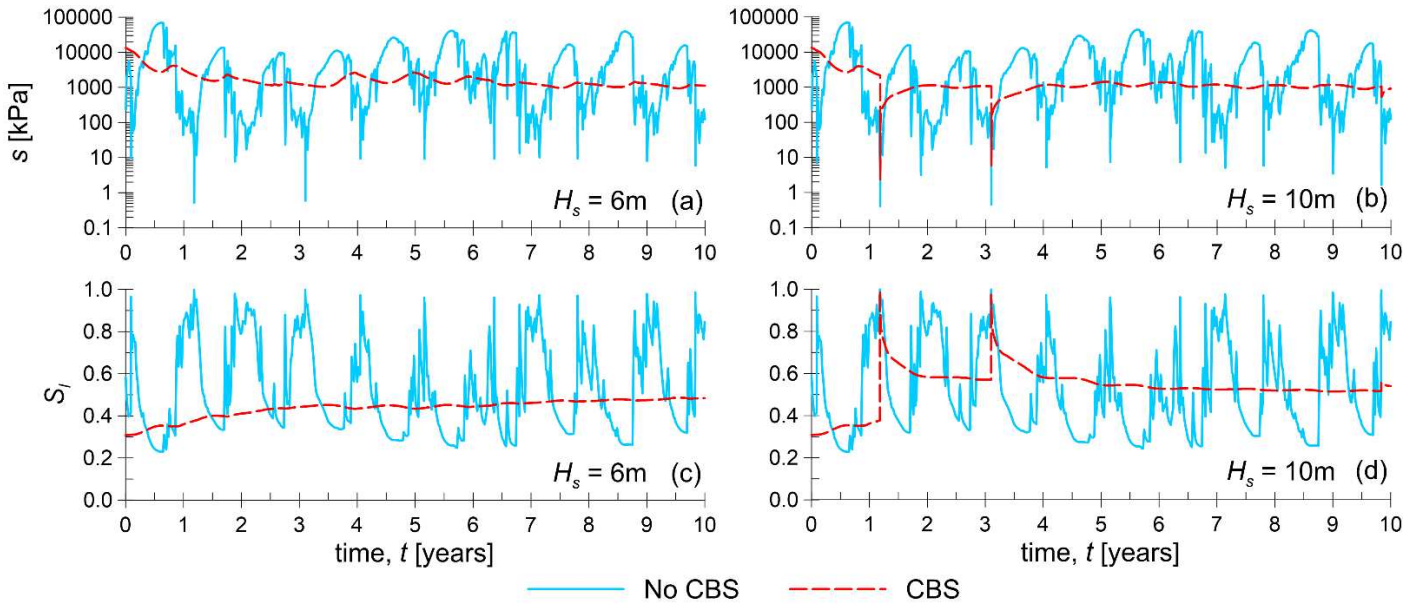

Fig. 6. Time histories of suction and degree of saturation in the underlying soil at the toe of the slope (point A) for different slope heights: (a,c) H_s = 6m, (b,d) H_s = 10m.

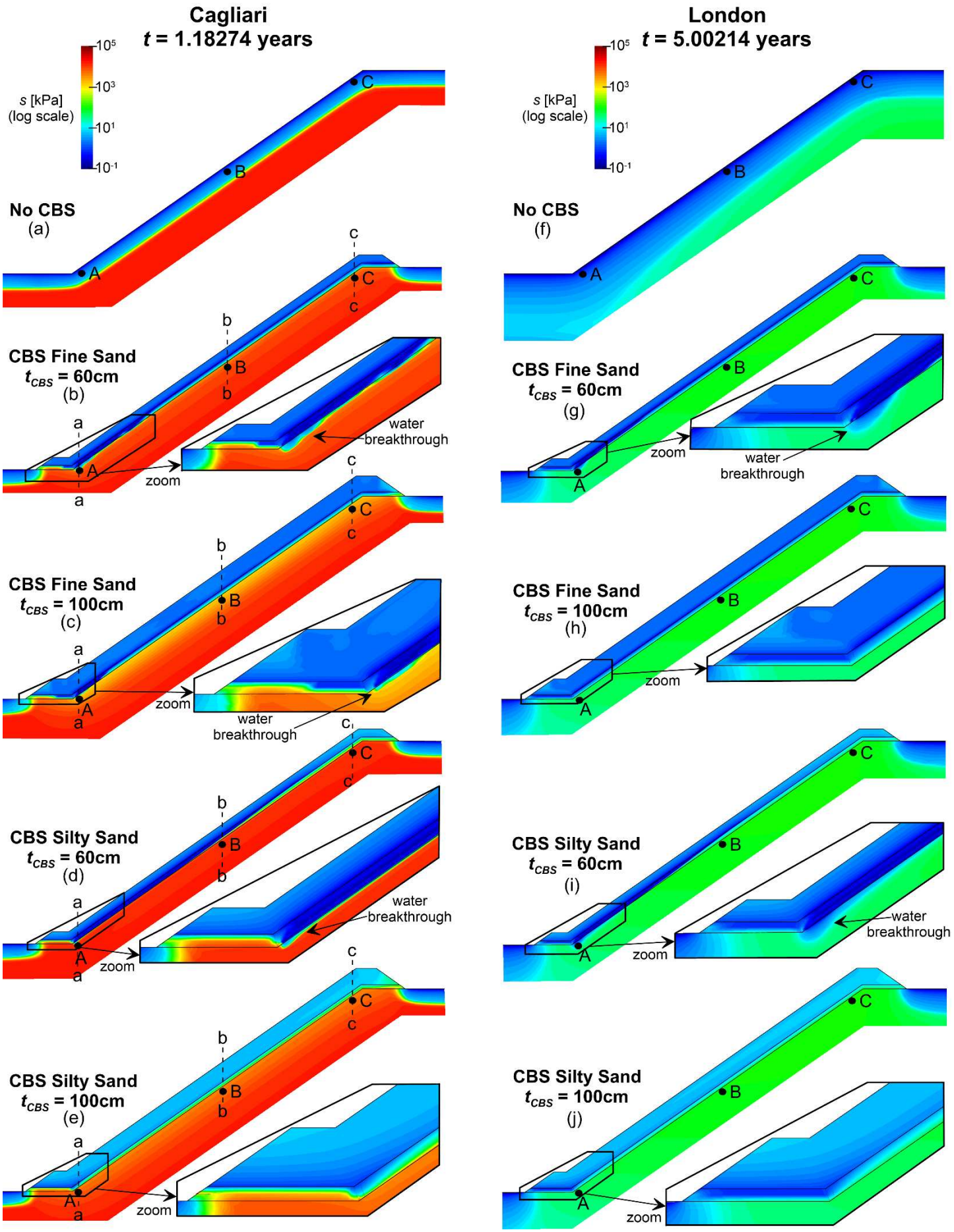

Fig. 7. Suction contours at the most critical rainfall event in Cagliari (t =1.18274 years) and London (t =5.00214 years) for the different models analysed.

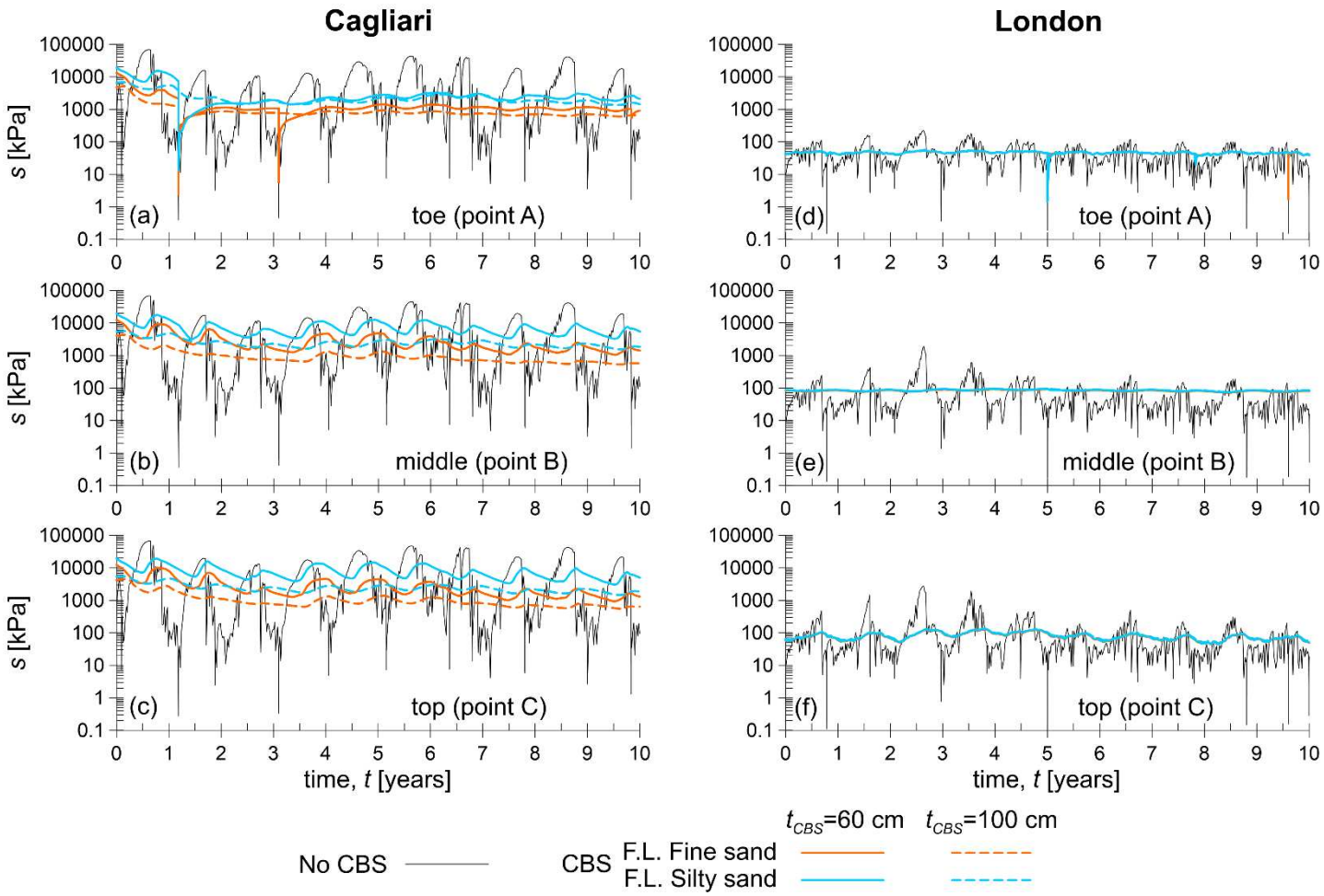

Fig. 8. Time histories of suction in Cagliari and London for the different models analysed.

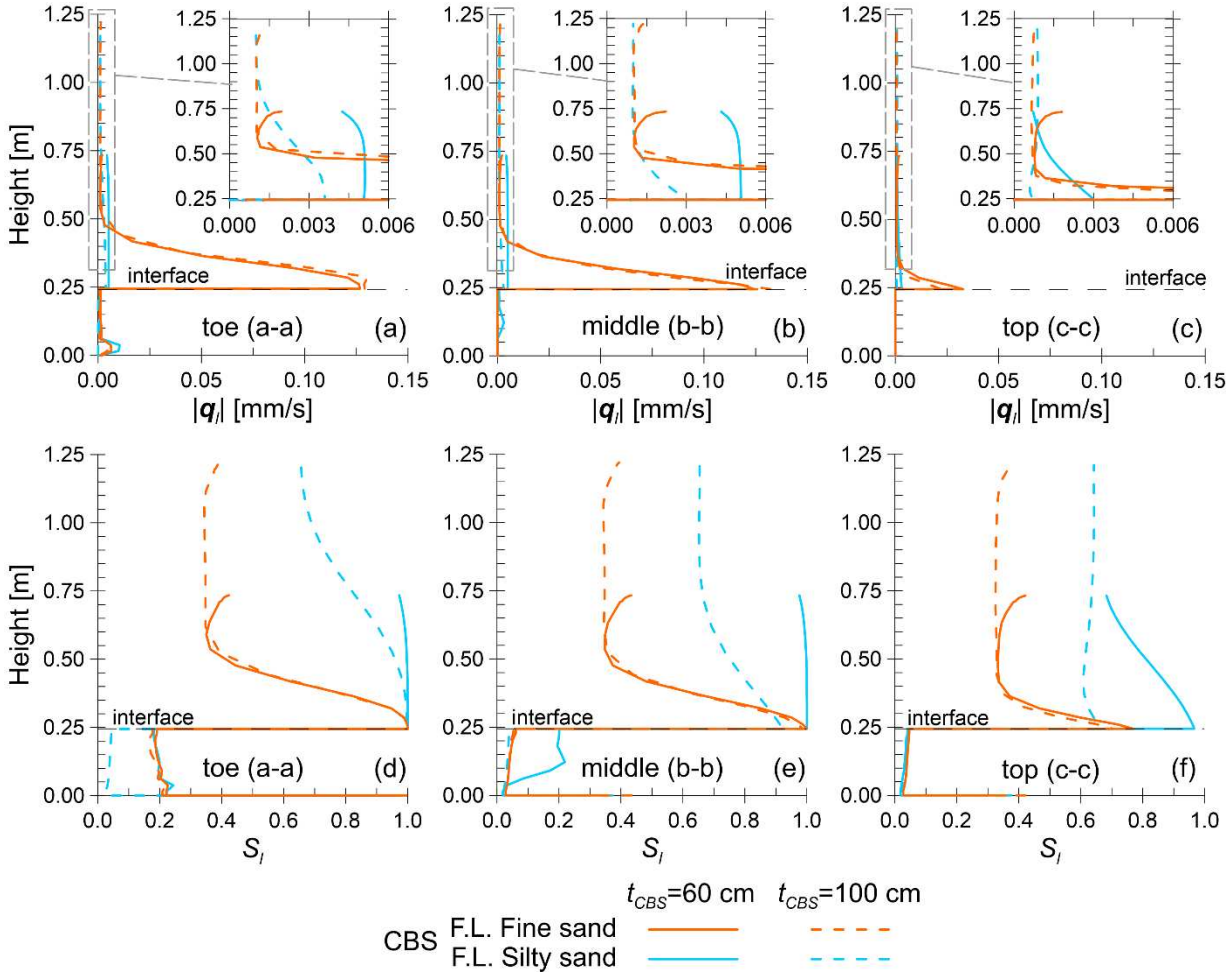

Fig. 9. Absolute liquid velocity (a-c) and degree of saturation (d-f) profiles at different sections in the CBS at the most critical rainfall event in Cagliari, i.e. t = 1.18274years, for different models.

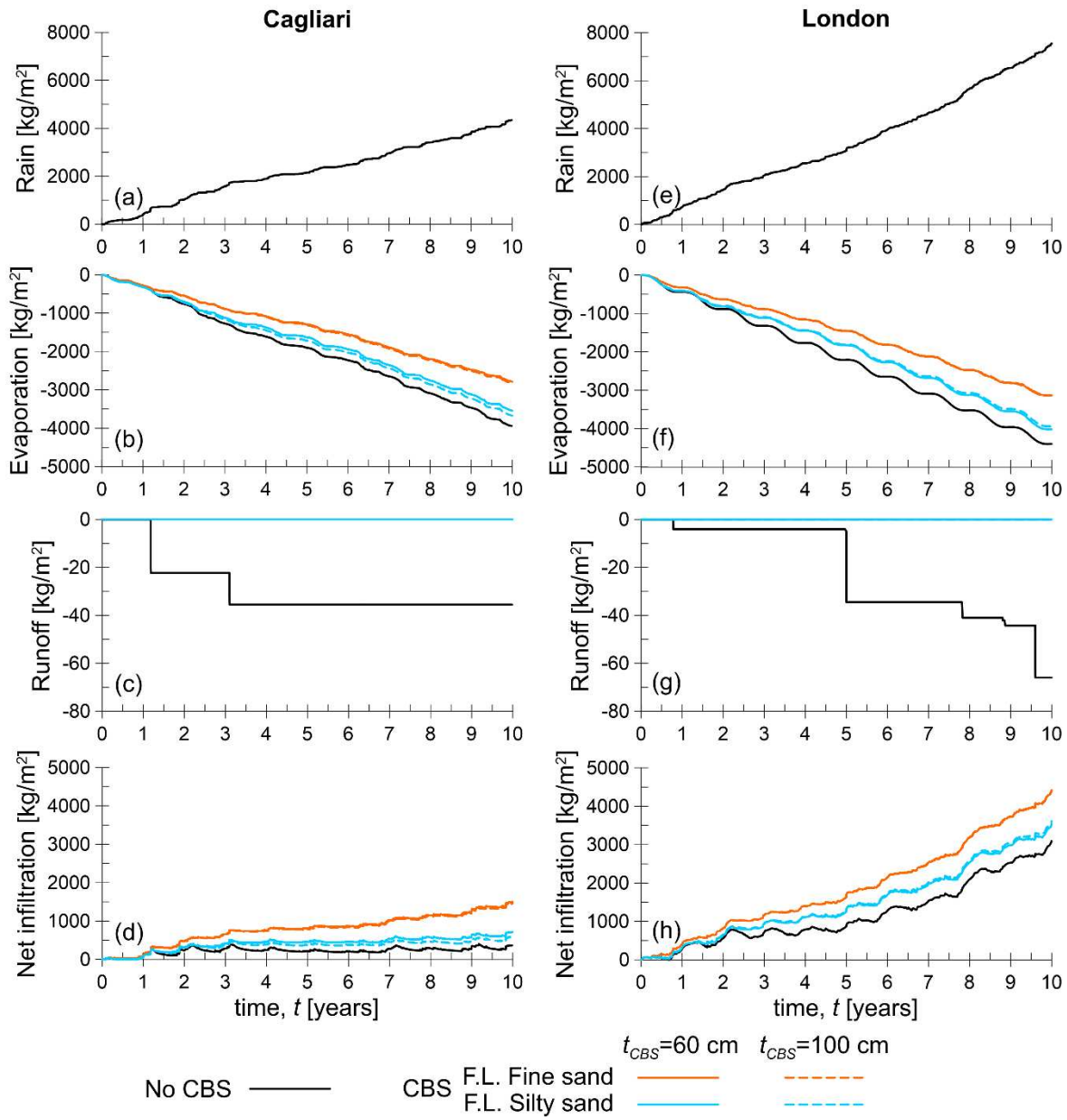

Fig. 10. Cumulative water flows at the top boundary surface of the different model analysed.

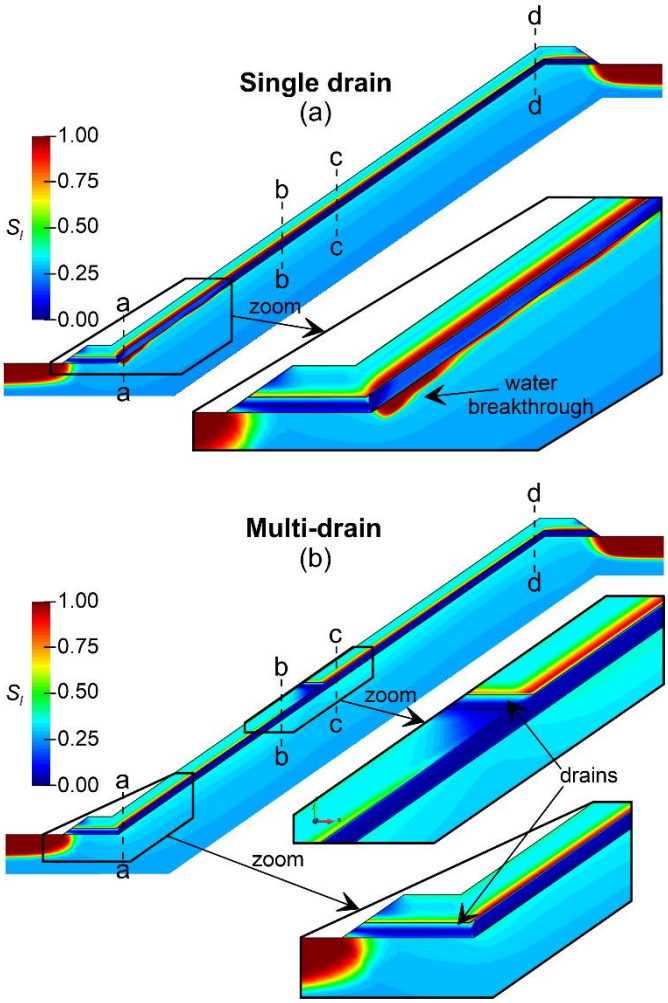

Fig. 11. Degree of saturation contours at the most critical rainfall event in Cagliari (t =1.18274 years) for the models with (a) a single drain and (b) multiple drains.

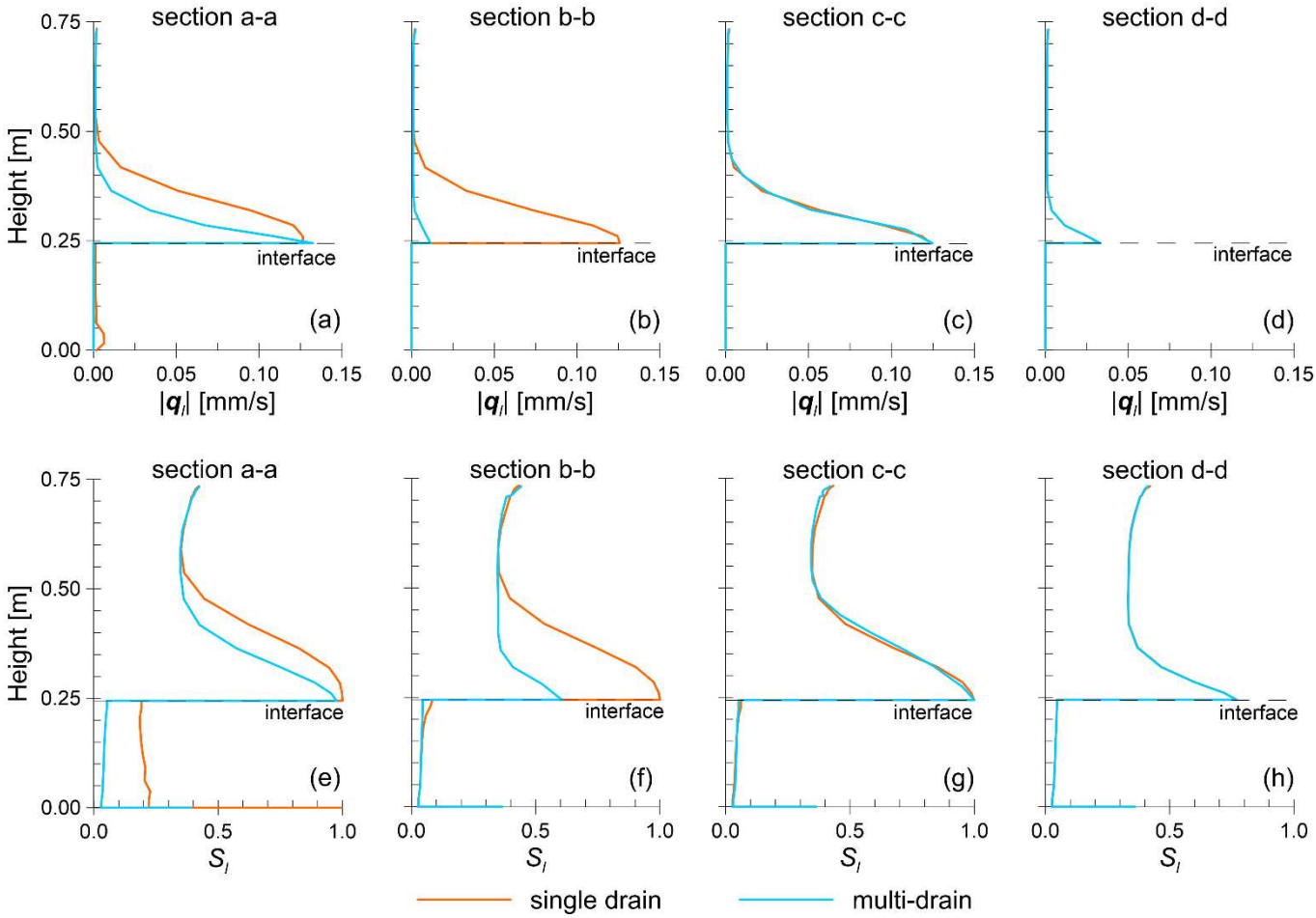

Fig. 12. (a-d) Absolute liquid velocity and (e-h) degree of saturation profiles at the end of the most critical rainfall event, i.e. t = 1.18274years, at four different sections for the single drain and multi-drain models.

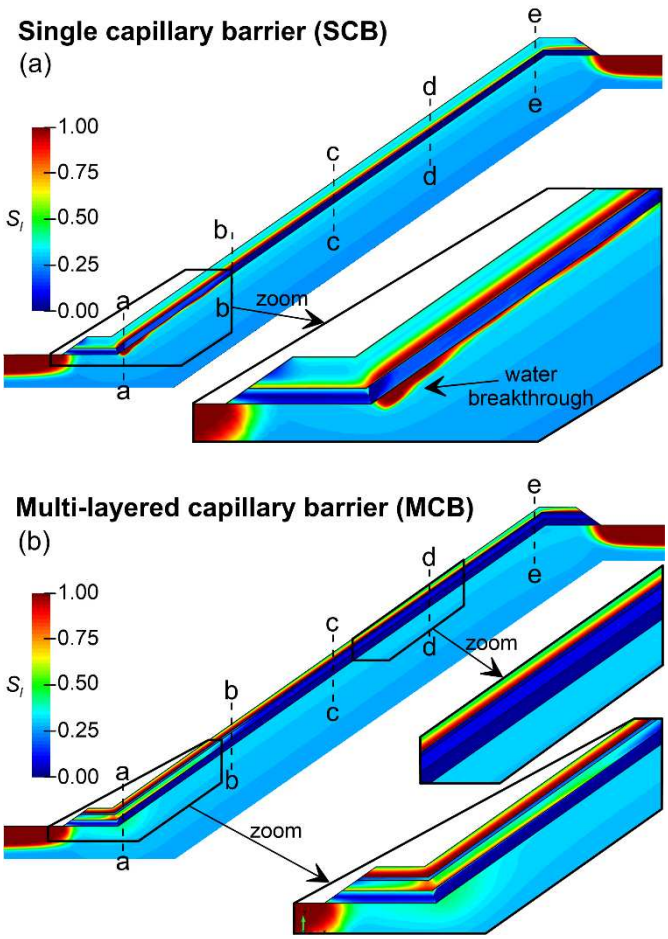

Fig. 13. Degree of saturation contours at the most critical rainfall event in Cagliari (t =1.18274 years) for the models with (a) a single CBS and (b) a multi-layered CBS.

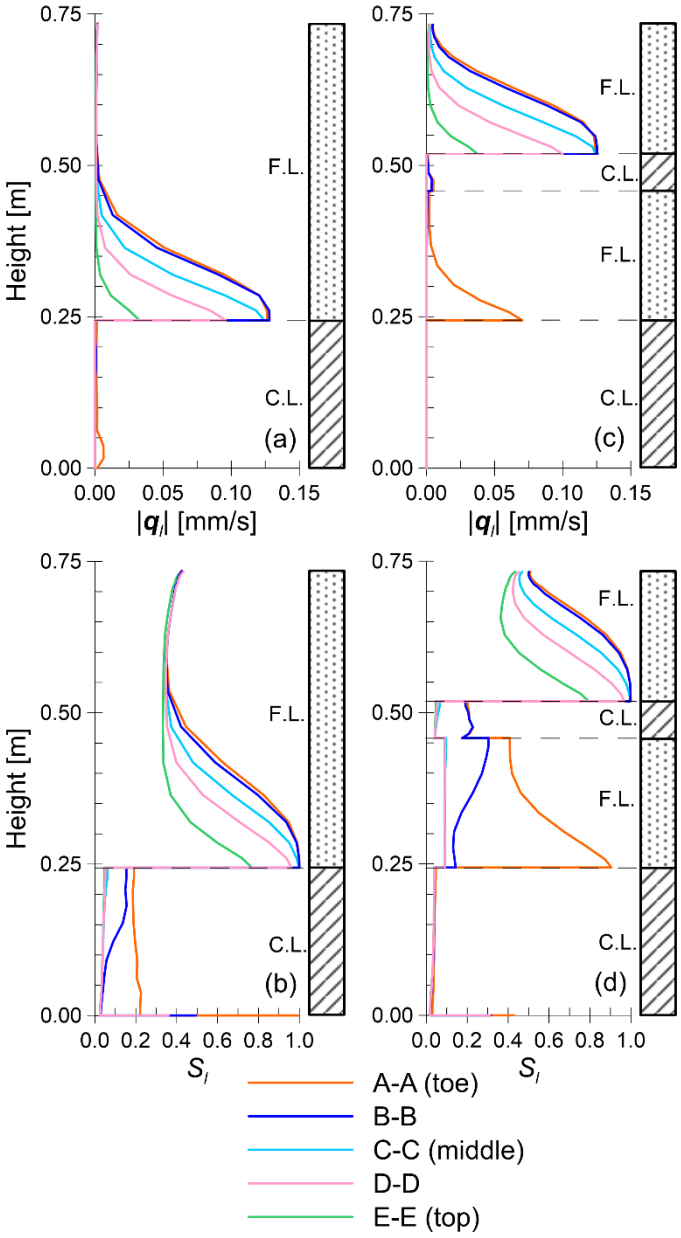

Fig. 14. (a,c) Absolute liquid velocity and (b,d) degree of saturation profiles at the end of the most critical rainfall event, i.e. t = 1.18274 years, at five different sections, (a,b) for the single CBS and (c,d) for the multi-layered CBS.

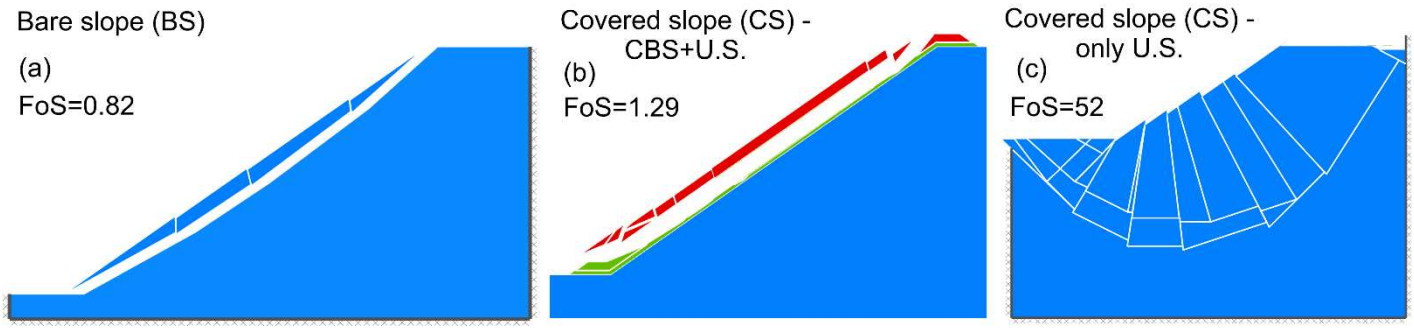

Fig. 15. Failure mechanisms at the most critical time in Cagliari, i.e. t = 1.18274years, for the models: (a) bare slope, (b) slope covered by the CBS (fine sand t_{CBS} = 60cm) and (c) underlying soil with hydraulic conditions of the slope covered by the CBS.

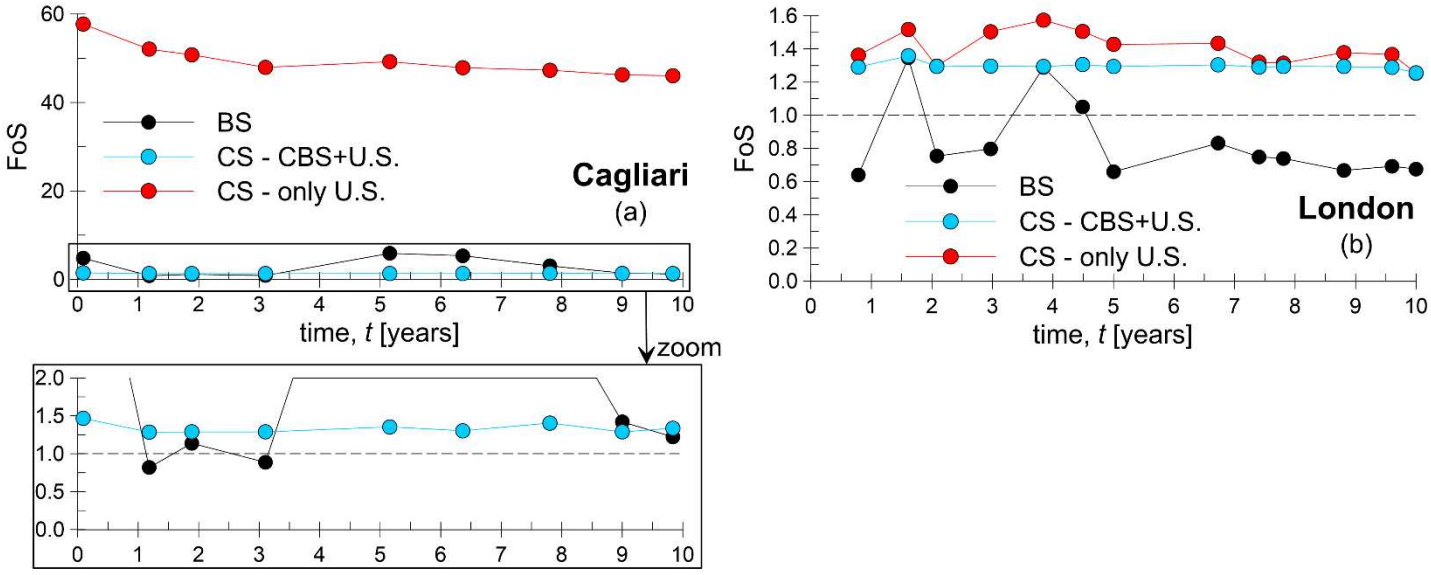

Fig. 16. Time histories of the factor of safety for the models for critical rainfall events in (a) Cagliari and (b) London: bare slope (BS), slope covered by the CBS (fine sand t_{CBS} = 60cm) (CS-CBS+U.S.) and underlying soil with hydraulic conditions of the slope covered by the CBS (CS-U.S.).

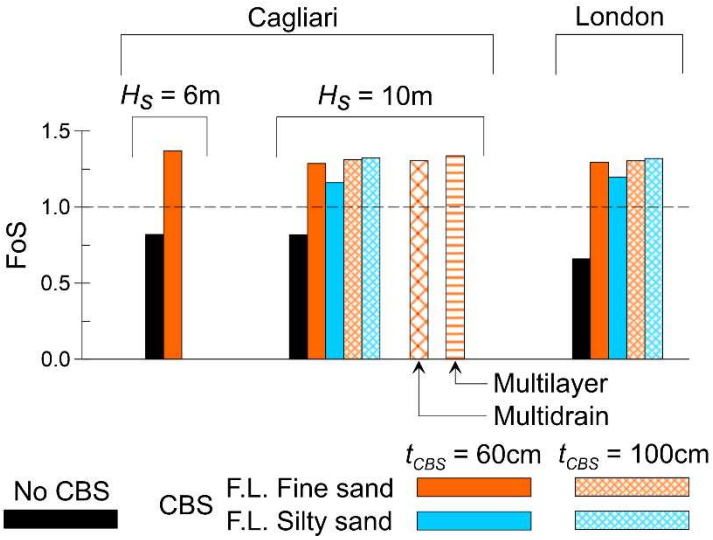

Fig. 17. Minimum factors of safety obtained for the models analyses.